
Regret Minimization Experience Replay in Off-Policy Reinforcement Learning

Xu-Hui Liu*, Zhenghai Xue*, Jing-Cheng Pang, Shengyi Jiang, Feng Xu, Yang Yu[†]

National Key Laboratory of Novel Software Technology

Nanjing University, Nanjing 210023, China

liuxh@lamda.nju.edu.cn, xuezh@smail.nju.edu.cn

{pangjc, jiangsy, xufeng}@lamda.nju.edu.cn, yuy@nju.edu.cn

Abstract

In reinforcement learning, experience replay stores past samples for further reuse. Prioritized sampling is a promising technique to better utilize these samples. Previous criteria of prioritization include TD error, recentness and corrective feedback, which are mostly heuristically designed. In this work, we start from the regret minimization objective, and obtain an optimal prioritization strategy for Bellman update that can directly maximize the return of the policy. The theory suggests that data with higher hindsight TD error, better on-policiness and more accurate Q value should be assigned with higher weights during sampling. Thus most previous criteria only consider this strategy partially. We not only provide theoretical justifications for previous criteria, but also propose two new methods to compute the prioritization weight, namely ReMERN and ReMERT. ReMERN learns an error network, while ReMERT exploits the temporal ordering of states. Both methods outperform previous prioritized sampling algorithms in challenging RL benchmarks, including MuJoCo, Atari and Meta-World.

1 Introduction

Reinforcement learning (RL) [1] has achieved great success in sequential decision making problems. Off-policy RL algorithms [2, 3, 4, 5, 6] have the ability to learn from a more general data distribution than on-policy counterparts, and often enjoy better sample efficiency. This is critical when the data collection process is expensive or dangerous. Experience Replay [7] enables data reuse and has been widely used in off-policy reinforcement learning. Previous work [8] points out that emphasizing on important samples in the replay buffer can benefit off-policy RL algorithms. Prioritized Experience Replay (PER) [9] quantifies such importance by the magnitude of temporal-difference (TD) error. Based on PER, many sampling strategies [10, 11, 12] are proposed to perform prioritized sampling. They are either based on TD error [9, 10, 12] or focused on the existence of corrective feedback [11]. However, these are all proxy objectives and different from the objective of RL, i.e., minimizing policy regret. They can be suboptimal in some cases due to this objective mismatch.

In this paper, we first give examples to illustrate the objective mismatch in previous prioritization strategies. Experiments show that lower TD error or more accurate Q function can not guarantee better policy performance. To tackle this issue, we first formulate an optimization problem that directly minimizes the regret of the current policy with respect to prioritization weights. We then make several approximations and solve this optimization problem. An optimal prioritization strategy is obtained and indicates that we should pay more attention to experiences with higher hindsight TD error, better on-policiness and more accurate Q value. To the best of our knowledge, this paper is the

*Equal contribution

[†]Corresponding author

first to optimize the sampling distribution of replay buffer theoretically from the perspective of regret minimization.

We then provide tractable approximations to the theoretical results. The on-policiness can be estimated by training a classifier to distinguish recent transitions, which are generally more on-policy, from early ones, which are generally more off-policy. The oracle Q value is inaccessible during training, so we can not calculate the accuracy of Q value directly. Inspired by DisCor [11], we propose an algorithm named ReMERN which estimates the suboptimality of Q value with an error network updated by Approximate Dynamic Programming (ADP).

ReMERN outperforms previous methods in environments with high randomness, e.g. with stochastic target positions or noisy rewards. However, the training of an extra neural network can be slow and unstable. We propose another estimation of Q accuracy based on a temporal viewpoint. With Bellman updates, the error in Q value accumulates from the next state to the previous one all across the trajectory. The terminal state has no bootstrapping target and low Bellman error. Therefore, states fewer steps away from the terminal state will have lower error in the updated Q value because of the more accurate Bellman target. This intuition is verified both empirically and theoretically. We then propose Temporal Correctness Estimation (TCE) based on the distance of each state to a terminal state, and name the overall algorithm ReMERT.

Similar to PER, ReMERN and ReMERT can be a plug-in module to all off-policy RL algorithms with a replay buffer, including but not limited to DQN [5] and SAC [2]. Experiments show that ReMERN and ReMERT substantially improve the performance of standard off-policy RL methods in various benchmarks.

2 Background

2.1 Preliminaries

A Markov decision process (MDP) is denoted $(\mathcal{S}, \mathcal{A}, T, r, \gamma, \rho_0)$, where \mathcal{S} is the state space, and \mathcal{A} is the action space. $T(s'|s, a)$ and $r(s, a) \in [0, R_{\max}]$ are the transition and reward function. $\gamma \in (0, 1)$ is the discounted factor and $\rho_0(s)$ is the distribution of the initial state. The target of reinforcement learning is to find a policy that maximizes the expected return: $\eta(\pi) = \mathbb{E}_\pi[\sum_{t \geq 0} \gamma^t r(s_t, a_t)]$, where the expectation is calculated from trajectories sampled from $s_0 \sim \rho_0$, $a_t \sim \pi(\cdot|s_t)$, and $s_{t+1} \sim T(\cdot|s_t, a_t)$ for $t \geq 0$.

For a fixed policy, an MDP becomes a Markov chain, where the discounted stationary state distribution is defined as $d^\pi(s)$. With a slight abuse of notation, the discounted stationary state-action distribution is defined as $d^\pi(s, a) = d^\pi(s)\pi(a|s)$. Then the expected return can be rewritten as $\eta(\pi) = \frac{1}{1-\gamma}\mathbb{E}_{d^\pi(s,a)}[r(s, a)]$. We assume there exists an optimal policy π^* such that $\pi^* = \arg \max_\pi \eta(\pi)$. We use the standard definition of the state-action value function, or Q function: $Q^\pi(s, a) = \mathbb{E}_\pi[\sum_{t \geq 0} \gamma^t r(s_t, a_t)|s_0 = s, a_0 = a]$. Let Q^* be the shorthand for Q^{π^*} . Q^* satisfies the Bellman equation $Q^*(s, a) = \mathcal{B}^*(Q^*(s, a))$, where $\mathcal{B}^* : \mathbb{R}^{\mathcal{S} \times \mathcal{A}} \rightarrow \mathbb{R}^{\mathcal{S} \times \mathcal{A}}$ is the Bellman optimal operator: $(\mathcal{B}^*f)(s, a) := r(s, a) + \gamma \max_{a'} \mathbb{E}_{s' \sim P(s,a)} f(s', a')$, where $f \in \mathbb{R}^{\mathcal{S} \times \mathcal{A}}$.

The regret of policy π is defined as $\text{Regret}(\pi) = \eta(\pi^*) - \eta(\pi)$. It measures the expected loss in return by following policy π instead of the optimal policy. Since $\eta(\pi^*)$ is a constant, minimizing the regret is equivalent to maximizing the expected return, and thus it can be an alternative objective of reinforcement learning.

2.2 Related Work

Extensive researches have been conducted on experience replay and replay buffer. The most frequently considered aspect is the sampling strategy. Various techniques have achieved good performance by performing prioritized sampling on the replay buffer. In model-based planning, Prioritized Sweeping [13, 14, 15] selects the next state updates according to changes in value. Prioritized Experience Replay (PER) [9] prioritizes samples with high TD error. Taking PER one step further, Prioritized Sequence Experience Replay (PSER) [10] considers information provided by transitions when estimating TD error. Emphasizing Recent Experience (ERE) [16] and Likelihood-Free Importance Weighting (LFIW) [12] prioritizes the correction of TD errors for frequently encountered states.

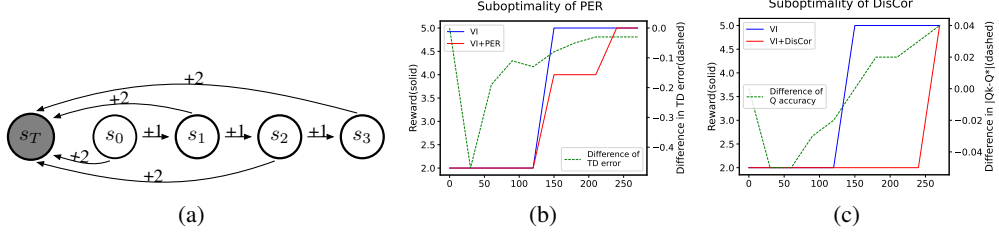


Figure 1: A simple MDP showing the objectives of PER and DisCor can slow down the training process. (a) A 5-state MDP with initial state s_0 and terminal state s_T . Except for s_3 and s_T , there are two available actions, *left* and *right*. Turning *left* leads to the terminal state s_T and +2 reward, while turning *right* leads to the next state and +1 reward. The optimal policy is to keep turning *right* until reaching s_3 , then reach s_T . (b) Relationship between TD error (dashed line) and performance (solid line) of VI and VI+PER. (c) Relationship between Q error (dashed line) and performance (solid line) of VI and VI+DisCor.

Distribution Correction (DisCor) [11] assigns higher weights to samples with more accurate target Q value because these samples provide “corrective feedback”. DisCor uses a neural network to estimate the accuracy of target Q value. Inspired by DisCor, SUNRISE [17] proposes to use the variance of ensembled Q functions as a surrogate for the accuracy of Q value. Adversarial Feature Matching [18] focuses on sampling uniformly among state-action pairs.

Instead of proposing a new strategy of sampling, [19] proves that there exists a relationship between sampling strategy and loss function, and weighted value loss can serve as a surrogate for prioritized sampling. Other works focus on buffer capacity [20, 21]. They point out that a proper buffer capacity can accelerate value estimation and lead to better learning efficiency and performance. In fact, this can be thought of as a specific example of prioritization strategies, i.e., assigning zero weights to the samples exceeding the proper buffer capacity.

3 Optimal Prioritization Strategy via Regret Minimization

3.1 Revisiting Existing Prioritization Methods

PER and DisCor are two representative algorithms of prioritized sampling. PER prioritizes state-action pairs with high TD error, while DisCor prefers to perform Bellman update on state-action pairs that have more accurate Bellman targets. However, both criteria are different from the target of RL algorithms, which is to maximize the expected return of the policy. Such difference can slow down the training process in some cases. For example, when the Bellman target is inaccurate, minimizing TD error does not necessarily improve the optimality of Q value.

To illustrate the aforementioned problems, we provide an example MDP shown in the left part of Fig. 1(a). This is a five-state MDP with two actions: turning *left* and *right*. The optimal policy is to turn *right* in all states, receiving a total reward of 5. Suppose the Q values for all (s, a) pairs are initialized to zero. The reward of turning *left* is higher than turning *right* in all states, so the *left* action has a higher TD error. As a result, PER prefers states with the *left* action, which is not the fastest training process to achieve the optimal policy. Also, since there is no bootstrapping error for the terminal state s_T , transitions with s_T as the next state have an accurate target Q value. Therefore, DisCor also focuses on state-actions pairs with *left* action, which is again not optimal.

We perform Value Iteration (VI) on this MDP. To simulate function approximation in Deep RL and avoid convergence in few iterations, the learning rate is set to 0.1. Prioritized sampling is substituted by weighted Bellman update, as introduced in [19]. The results are shown in Fig. 1(b) and Fig. 1(c). According to the results, PER indeed minimizes TD error more efficiently, and DisCor results in a more accurate estimation of Q value, as indicated by their objectives. However, they both need more iterations to converge than value iteration without prioritization. According to this MDP, the objective of previous prioritization methods can be inefficient in certain cases.

3.2 Problem Formulation of Regret Minimization

As shown in Section 3.1, an indirect objective can cause slower convergence of value iteration. In this section, we aim to find an optimal prioritization weight w_k that can directly minimize the policy regret $\eta(\pi^*) - \eta(\pi_k)$. The weight is multiplied to the Bellman error $(Q - \mathcal{B}^* Q_{k-1})^2$ and π_k can be obtained from the updated Q function. To facilitate further derivations, we only consider the best Q function of the Bellman update, which is calculated by the arg min operator. Therefore, the optimization problem with respect to w_k can be written as:

$$\begin{aligned} \min_{w_k} \quad & \eta(\pi^*) - \eta(\pi_k) \\ \text{s.t.} \quad & Q_k = \arg \min_{Q \in \mathcal{Q}} \mathbb{E}_\mu[w_k(s, a) \cdot (Q - \mathcal{B}^* Q_{k-1})^2(s, a)], \\ & \mathbb{E}_\mu[w_k(s, a)] = 1, \quad w_k(s, a) \geq 0, \end{aligned} \quad (1)$$

where $\pi_k(s) = \frac{\exp(Q_k(s, a))}{\sum_{a'} \exp(Q_k(s, a'))}$ is the policy corresponding to Q_k . \mathcal{Q} is the function space of Q functions and μ is the data distribution of the replay buffer. Q_k is the estimate of Q value after the Bellman update at iteration k .

We then manage to solve this optimization problem. To get started, we introduce *recurring probability* which serves as an upper bound of the error term in our solution.

Definition 1 (Recurring Probability). *The recurring probability of a policy π is defined as $\epsilon_\pi = \sup_{s, a} \sum_{t=1}^{\infty} \gamma^t \rho^\pi(s, a, t)$, where ρ is the probability of the agent starting from (s, a) and coming back to s at time step t under policy π , i.e., $\rho^\pi(s, a, t) = \Pr(s_0 = s, a_0 = a, s_t = s, s_{1:t-1} \neq s; \pi)$.*

We then present the solution to the optimization problem 11 in Thm. 3. The formal version of the theorem and detailed proof are in Appendix A.

Theorem 1 (Informal). *Under mild conditions, the solution w_k to a relaxation of the optimization problem 11 in MDPs with discrete action spaces is*

$$w_k(s, a) = \frac{1}{Z_1^*} (E_k(s, a) + \epsilon_{k,1}(s, a)). \quad (2)$$

In MDPs with continuous action spaces, the solution is

$$w_k(s, a) = \frac{1}{Z_2^*} (F_k(s, a) + \epsilon_{k,2}(s, a)). \quad (3)$$

where

$$\begin{aligned} E_k(s, a) &= \underbrace{\frac{d^{\pi_k}(s, a)}{\mu(s, a)}}_{(a)} \underbrace{(2 - \pi_k(a|s))}_{(b)} \underbrace{\exp(-|Q_k - Q^*|(s, a))}_{(c)} \underbrace{|Q_k - \mathcal{B}^* Q_{k-1}|(s, a)}_{(d)} \\ F_k(s, a) &= 2 \underbrace{\frac{d^{\pi_k}(s, a)}{\mu(s, a)}}_{(a)} \underbrace{\exp(-|Q_k - Q^*|(s, a))}_{(c)} \underbrace{|Q_k - \mathcal{B}^* Q_{k-1}|(s, a)}_{(d)}, \end{aligned}$$

Z_1^* , Z_2^* are normalization factors, $\epsilon_{k,1}(s, a)$ and $\epsilon_{k,2}(s, a)$ satisfy $\max \left\{ \frac{\epsilon_{k,1}(s, a)}{E_k(s, a)}, \frac{\epsilon_{k,2}(s, a)}{F_k(s, a)} \right\} \leq \epsilon_{\pi_k}$.

With regard to the error terms, there are two cases where ϵ_{π_k} is low by its definition: the probability of coming back to the states that have been visited is small, or the number of steps an agent takes to come back to the visited states is large. In most tasks, either of these cases holds. We conduct experiments in several Atari games and show the verification results in Appendix D. The low probability leads to small ϵ_{π_k} and implies the terms $\epsilon_{k,1}(s, a)$ and $\epsilon_{k,2}(s, a)$ are negligible.

Therefore, Thm. 3 suggests that state-action tuples in the replay buffer should be assigned with higher importance if they have the following properties:

- **Higher hindsight Bellman error** (from $|Q_k - \mathcal{B}^* Q_{k-1}|(s, a)$). Q_k is the estimate of Q value after the Bellman update. This term describes the difference between the estimated hindsight Q value and the Bellman target. It is similar to the prioritization criterion of PER [9], but PER concerns more about the historical Bellman error, i.e., $|Q_{k-1} - \mathcal{B}^* Q_{k-2}|(s, a)$.

- **More on-policiness** (from $\frac{d^{\pi_k}(s,a)}{\mu(s,a)}$). An efficient update of π requires w_k to be on-policy, i.e., focusing on state-action pairs which are more likely to be visited by the current policy. Such prioritization strategy has been empirically illustrated in LFIW [12] and BCQ [22], while we obtain it directly from our theorem.
- **Closer value estimation to oracle** (from $\exp(-|Q_k - Q^*(s, a)|)$). This term indicates that state-action pairs with less accurate Q values after the Bellman update should be assigned with lower weights. Intuitively, state-action pairs that lead to suboptimal updates of the estimator of Q value should be down-weighted. Such suboptimality may arise from incorrect target Q values or the error of function approximation in deep Q networks.
- **Smaller action likelihood** (from $2 - \pi_k(a|s)$). This term only exists in MDPs with a discrete action space. It offsets the effect of the on-policy term d^{π_k} to some extent and is similar to ε -greedy strategy in exploration.

Our theoretical analysis indicates that existing prioritization strategies only consider the problem partially, neglecting other terms in minimizing the regret. For example, DisCor fails to consider the on-policiness and PER ignores the accuracy of Q value. In the remaining part of this section, we present practical approximations to each term in Eq. (30) and (31).

Term (a) is the importance weight between the current policy and the behavior policy. We can calculate this term using Likelihood-Free Importance Weighting (LFIW, [12]). LFIW divides the replay buffer into two parts, a fast buffer \mathcal{D}_f and a slow buffer \mathcal{D}_s . It initializes a neural network $\kappa_\psi(s, a)$ and optimizes the network according to the following loss function:

$$L_\kappa(\psi) := \mathbb{E}_{\mathcal{D}_s} [f^*(f'(\kappa_\psi(s, a)))] - \mathbb{E}_{\mathcal{D}_f} [f'(\kappa_\psi(s, a))], \quad (4)$$

where f' and f^* is the derivative and convex conjugate of function f . The updated κ_ψ is the desired importance weight.

For term (b) and (d), since π_k and Q_k are the policy and the estimate of Q value after the update, they cannot be calculated directly. Therefore, we approximate them by the upper and lower bounds. For term (b), $1 \leq 2 - \pi_k(a|s) \leq 2$. For term (d), a viable approximation is to bound it between the minimum and maximum Bellman errors obtained at the previous iteration, $c_1 = \min_{s,a} |Q_{k-1} - \mathcal{B}^* Q_{k-2}|$ and $c_2 = \max_{s,a} |Q_{k-1} - \mathcal{B}^* Q_{k-2}|$. As shown in DisCor, we can restrict the support of state-action pairs (s, a) used to compute c_1 and c_2 in the support of replay buffer, to ensure that both c_1 and c_2 are finite. With these approximation, we can derive a lower bound for w_k , which will be detailed in Sec. 3.3 and Sec. 3.4.

In the next two subsections, we will provide two practical algorithms to estimate $|Q_k - Q^*|$.

3.3 Regret Minimization Experience Replay Using Neural Network (ReMERN)

DisCor shows Δ_k can be a surrogate of $|Q_k - Q^*|$, which is defined as:

$$\Delta_k = \sum_{i=1}^k \gamma^{k-i} \left(\prod_{j=i}^{k-1} P^{\pi_j} \right) |Q_i - \mathcal{B}^* Q_{i-1}| \quad (5)$$

$$\implies \Delta_k = |Q_k - \mathcal{B}^* Q_{k-1}| + \gamma P^{\pi_{k-1}} \Delta_{k-1} \quad (6)$$

According to Eq. (6), $\gamma[P^{\pi_{k-1}} \Delta_{k-1}](s, a) + c_2$ is an upper bound of $|Q_k - Q^*|$. This is because Δ_k is proven to be the upper bound of $|Q_k - Q^*|$ [11] and c_2 is the upper bound of $|Q_k - \mathcal{B}^* Q_{k-1}|$. Recall that $2 - \pi_k(a|s) \geq 1$ and $|Q_{k-1} - \mathcal{B}^* Q_{k-2}| \geq c_1$, and we can derive the final expression for this tractable approximation for $w_k(s, a)$ by simplifying all constants:

$$w_k(s, a) \propto \frac{d^{\pi_k}(s, a)}{\mu(s, a)} \exp(-\gamma [P^{\pi_{k-1}} \Delta_{k-1}](s, a)), \quad (7)$$

This approximation applies to MDPs with discrete action space and MDPs with continuous action space. Using the lower bound of $w_k(s, a)$ may down-weight some transitions, but will never up-weight a transition by mistake [11].

We use a neural network to estimate Δ_{k-1} . As shown in Eq. (6), Δ_{k-1} can be calculated from a bootstrapped target, which inspires us to use ADP algorithms to update it. We name this method

ReMERN (**R**egret **M**inimization **E**xperience **R**eplay using **N**eural Network). The pseudo code for ReMERN is presented in Appendix C. ReMERN is applicable to all value-based off-policy algorithms with replay buffer.

3.4 Regret Minimization Experience Replay Using Temporal Structure (ReMERT)

ReMERN uses neural network as the estimator of $|Q_k - Q^*|$. However, training a neural network is time consuming and suffers from large estimation error without adequate iterations. To mitigate this issue, we propose another estimation of $|Q_k - Q^*|$ from a different perspective.

3.4.1 The Temporal Property of Q Error

$|Q_k - Q^*|$ can be decomposed with the triangle inequality: $|Q_k - Q^*| \leq |Q_k - \mathcal{B}^* Q_{k-1}| + |\mathcal{B}^* Q_{k-1} - Q^*|$. The first term is the projection error depending on the Q function space \mathcal{Q} . This error is usually small thanks to the strong expressive power of neural networks. In the second term, $\mathcal{B}^* Q_{k-1}$ is the estimate of target Q value, and $|\mathcal{B}^* Q_{k-1} - Q^*|$ is the distance from the target Q value to the ground-truth Q value. The target Q value at the terminal state consists of the reward only, so there is no bootstrapping error and $|\mathcal{B}^* Q_{k-1} - Q^*| = 0$. Moving backward through the trajectory, the accuracy of the Q value estimation decreases as the error of Bellman update accumulates. These Q values are then utilized to compute the target Q value, leading to more erroneous Bellman updates and larger $|\mathcal{B}^* Q_{k-1} - Q^*|$. Such error can accumulate through the MDP. Consequently, states closer to the terminal state tend to have a more accurate Bellman target. This motivates us to estimate the incorrectness of the estimated Q value using the temporal information of a given state-action tuple (s_t, a_t) .

To verify our intuition on the temporal property of Q error, we use a gridworld MDP from [23] and visualize the mean error of the target Q value (i.e., $|\mathcal{B}^* Q_{k-1} - Q^*|$) across different actions in Fig. 2. We use DQN to update Q values. In this gridworld MDP, an agent starts at the red triangle on the top-left and terminates at the green rectangle on the top-right. The agent can't go through the wall, which is plotted as gray grids. The darker a grid is, the higher error of Q function it has. This figure illustrates that states closer to the terminal state has lower Q error, corresponding to our intuition that $|\mathcal{B}^* Q_{k-1} - Q^*|$ is related to the position of (s, a) in the trajectory.

To formalize this intuition, we first define *Distance to End*.

Definition 2 (Distance to End). *Given a MDP \mathcal{M} , $\tau = \{s_t, a_t\}_{t=0}^T$ is a trajectory generated by policy π in \mathcal{M} . The distance to end of (s_t, a_t) , denoted by $h_\tau^\pi(s_t, a_t)$, is $T - t$ in this trajectory.*

Our intuition states that the value of $|Q_k - Q^*|$ has a positive correlation with distance to end. Based on this intuition, we propose the following theorem.

Theorem 2 (Informal). *Under mild conditions, with probability at least $1 - \delta$, we have*

$$\begin{aligned} & |Q_k(s, a) - Q^*(s, a)| \\ & \leq \mathbb{E}_\tau \left(f(h_\tau^{\pi_k}(s, a)) (L_{Q_{k-1}} + c) + \gamma^{h_\tau^{\pi_k}(s, a)+1} c \right) + g(k, \delta) \end{aligned} \tag{8}$$

where $c = \max_{s, a} (Q^*(s, a^*) - Q^*(s, a))$, $f(t) = \frac{\gamma - \gamma^t}{1 - \gamma}$, $L_{Q_{k-1}} = \mathbb{E}[|Q_{k-1} - \mathcal{B}^* Q_{k-2}|]$ and $g(k, \delta)$ decreases exponentially as k increases.

The formal version of the theorem and its proof are in Appendix B. The theorem states that $|Q_k - Q^*|$ is upper bounded by a function of distance to end and expected Bellman error with high probability.

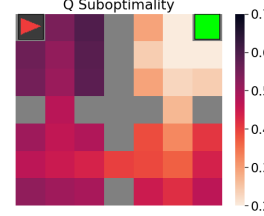


Figure 2: The visualized error of target Q value in a GridWorld Environment. The Q error is visualized by the color of the grid.

3.4.2 A Practical Implementation

In Thm. 2 we derive the upper bound of $|Q_k - Q^*|$, which can serve as a surrogate to $|Q_k - Q^*|$. Using an upper bound as the surrogate may down-weight some transitions, but will never up-weight a transition that should not be up-weighted [11]. We call this Temporal Correctness Estimation (TCE):

$$\begin{aligned} |Q_k(s, a) - Q^*(s, a)| &\approx \mathbb{E}_\tau \text{TCE}_c(s, a) \\ &= \mathbb{E}_\tau \left(f(h_\tau^{\pi_{k-1}}(s, a)) (L_{Q_{k-1}} + c) + \gamma^{h_\tau^{\pi_{k-1}}(s, a)+1} c \right), \end{aligned} \quad (9)$$

Similar to the derivation of ReMERN, we can simplify the expression of $w_k(s, a)$ as:

$$w_k(s, a) \propto \frac{d^{\pi_k}(s, a)}{\mu(s, a)} \exp \left(-\mathbb{E}_\tau \text{TCE}_c(s, a) \right) \quad (10)$$

This approach of computing prioritization weights is named ReMERT (**R**egret **M**inimization **E**xperience **R**eplay using **T**emporal **S**tructure). Its pseudo code is presented in Appendix C. In practice, we record the *distance to end* of a state-action pair when it is sampled by the policy and stored in the replay buffer. The expectation with respect to τ is computed based on the record and Monte-Carlo estimation.

3.5 Comparison between ReMERN and ReMERT

ReMERT can estimate $|Q_k - Q^*|$ directly from the temporal ordering of states, which often provides more efficient and more accurate estimation than ReMERN. However, The expectation with respect to trajectory τ in Eq. (10) induces statistical error. In some environments, the *distance to end* of a certain state-action pair (s, a) can vary widely across different trajectories, which is usually caused by the randomness of environments. For example, in environments with stochastic goal positions, the state may be near the goal in one episode but far away from it in another. In such cases, prioritization weights provided by ReMERT have large variance and can be misleading. In contrast, ReMERN need to train an error net but is irrelevant to the *distance to end*. Therefore, ReMERN suffers estimation error of neural network but is robust to the randomness of environments. We test their property in the following section.

4 Experiments

In this section, we conduct experiments to evaluate ReMERN and ReMERT³. We choose SAC and DQN as the baseline algorithms for continuous and discrete action space respectively and incorporate ReMERN and ReMERT as the sampling strategy. We first compare the performance of ReMERN and ReMERT to prior sampling methods in continuous control benchmarks including Meta-World [24], MuJoCo [25] and Deepmind Control Suite (DMC) [26]. We also evaluate our methods in Arcade Learning Environments with discrete action spaces. Then, we dive into our algorithms and design several experiments, such as Gridworld tasks and MuJoCo with reward noise, to demonstrate some key properties of ReMERN and ReMERT. A detailed description of the environments and experimental details are listed in Appendix D.

4.1 Performance on Continuous Control Environments

In MuJoCo and DMC tasks, ReMERT outperforms baseline methods on four of six tasks and achieves comparable performance in the rest two tasks, i.e. HalfCheetah and Hopper, as shown in Fig. 3. The marginal improvement of ReMERT in HalfCheetah mainly comes from the absence of a strong correlation between Q-loss and time step. In HalfCheetah, there is no specific terminal state, so the agent always reaches the max length of the trajectory, which gives a fake "distance to end" for every state. In Hopper, there is not much difference of the $|Q_k - Q^*|$ term between all the sampled state-action pairs, as shown in Appendix D, so the state-action pairs are not sampled very unequally. Besides, Hopper is a relatively easy task, in which prioritizing the samples have minor impact on the

³Codes are available at <https://github.com/AIDefender/ReMERN-ReMERT>.

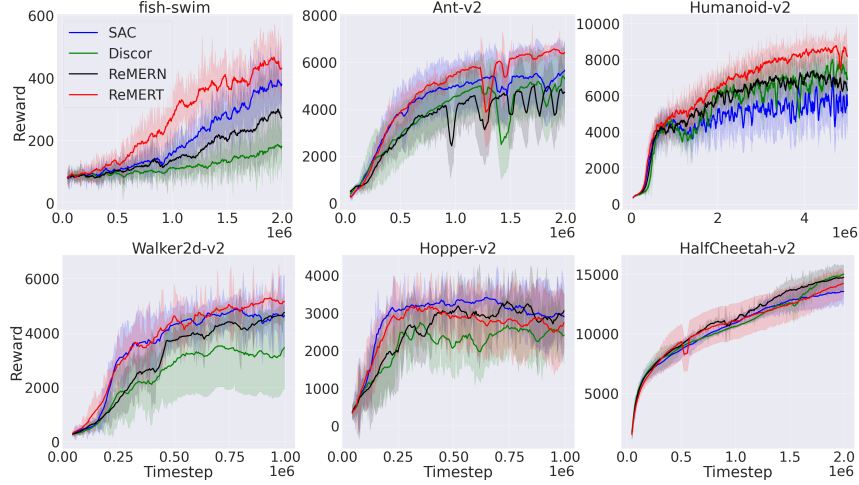


Figure 3: Performance of ReMERT, ReMERN with SAC and DisCor as baselines on continuous control tasks.

overall performance of the RL algorithm. The performance of ReMERN is better than DisCor, but is not as good as ReMERT. This verifies our theory and the existence of large estimation error induced by updating neural network with ADP algorithms.

The Meta-World benchmark [24] includes many robotic manipulation tasks. We select 8 tasks for evaluation, and plot the result in Fig. 4. The performance of PER can be found in its paper [9]. Current state-of-the-art off policy RL algorithms such as SAC performs poorly on this benchmark because the goals of tasks have high randomness. Although DisCor [11] shows preferable performance in these tasks compared to SAC and PER, ReMERN obtains a significant improvement over DisCor in the training speed and asymptotic performance. In this evaluation, we exclude ReMERT for comparison because the randomized target position in Meta-World contradicts its assumption.

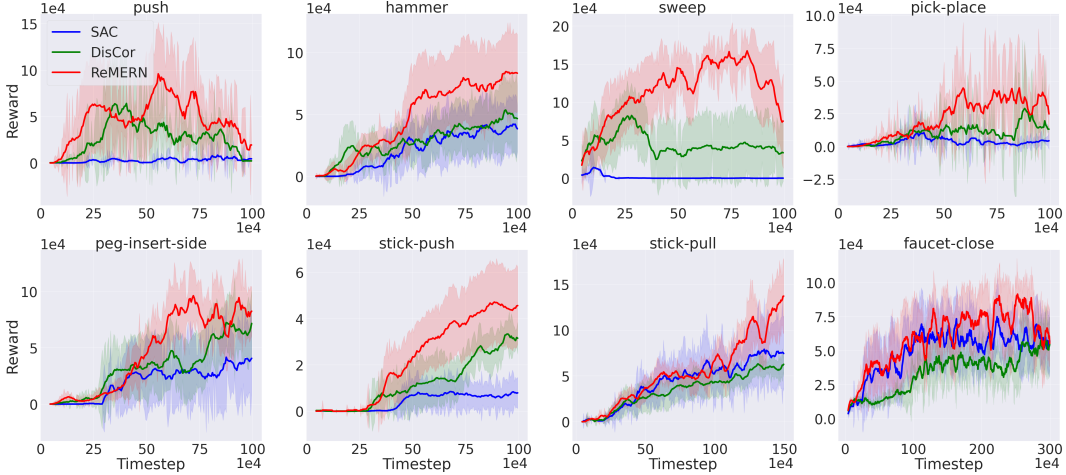


Figure 4: Performance of ReMERN, standard SAC and DisCor in eight Meta-World tasks. From left to right: push, hammer, sweep, peg-insert-side, stick push, stick pull, faucet close.

4.2 Performance on Arcade Learning Environments

Atari games are suitable for verifying our theory for MDPs with discrete action space. The tested games have a relatively stable temporal ordering of states because the initial state and the terminal state have little randomness, so that the assumption of ReMERT is satisfied. As shown by Tab. 1, ReMERT outperforms DQN in all the selected games. The results also suggest that ReMERT can be

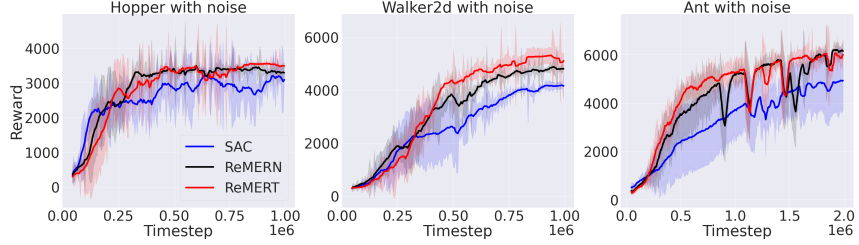


Figure 5: Performance of ReMERN, ReMERT and SAC on three continuous control tasks with reward noise.

applied to environments with high dimensional state spaces. Results of more Atari games are listed in Appendix D. We do not include ReMERN for comparison because DisCor which is a composing part of ReMERN has no open-source code available for discrete action space.

4.3 Demonstration on Key Properties of ReMERN and ReMERT

4.3.1 Influence of Environment Randomness

Fig. 3 and Fig. 4 show that ReMERN has a better performance on Meta-World than on Mujoco tasks. We attribute this to the robustness of our strategy in environments with high randomness. For a highly stochastic environment, the estimation of Q value is difficult. When the estimation of Q value is inaccurate, the target Q value is also inaccurate, leading to a suboptimal update process in off-policy RL algorithms. Thanks to the closer value estimation to oracle principle, ReMERN estimates the Q value more accurately than other methods. However, for less stochastic environments like MuJoCo environments, the accuracy of error network might become the bottleneck of ReMERN.

To show this empirically, we add Gaussian noise to the reward function in MuJoCo environments. The details of the experimental setup are listed in Appendix D. Fig. 5 show that: (1) ReMERN and ReMERT perform better than SAC in stochastic environments, which verifies our analysis. (2) Though ReMERT suffers statistical error of temporal ordering, it is robust to the randomness of reward because the temporal property is not affected by the noise.

4.3.2 Analysis of TCE on Deterministic Tabular Environments

To analyze the effect of the principle behind TCE, we evaluate the Q error in Gridworld with image input. We plot the $|Q_k - Q^*|$ error of standard DQN, DQN with DisCor, DQN with TCE and DQN with oracle at some time in the training process in Fig. 6. TCE is combined with DQN to estimate term (c) in Eq. (30), and the other terms are ignored to compute w_k . DQN with oracle uses the ground-truth error $|Q_k - Q^*|$ to calculate the prioritization weight. The result shows that DQN with TCE achieves a more accurate Q value estimator than those of standard DQN and DQN with DisCor, while DQN with oracle $|Q_k - Q^*|$ achieves the most accurate Q value estimator. The lower efficiency of DQN with DisCor is due to the slower convergence speed of the error network. This

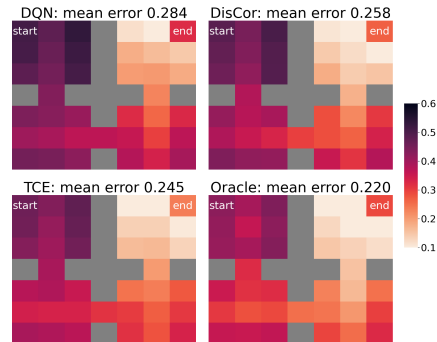


Figure 6: TCE and DisCor in Gridworld

Table 1: DQN vs ReMERT on Atari. DQN (Nature) is the performance in the DQN paper [5]. DQN (Baseline) is the performance of our baseline program [27].

Method	Enduro	KungFuMaster	Kangaroo	MsPacman	Qbert
DQN (Nature)	301 ± 24.6	23270 ± 5955	6740 ± 2959	2311 ± 525	10596 ± 3294
DQN (Baseline)	1185 ± 100	29147 ± 7280	6210 ± 1007	3318 ± 647	13437 ± 2537
ReMERT (Ours)	1303 ± 258	35544 ± 8432	7572 ± 1794	3481 ± 1351	14511 ± 1138

proves the principle behind our theory effective, and TCE is a decent approximation of $|Q_k - Q^*|$.

5 Conclusion and Future Work

In this work, we first revisit the existing methods of prioritized sampling and point out that the objectives of these methods are different from the objective of RL, which can lead to a suboptimal training process. To solve this issue, we analyze the prioritization strategy from the perspective of regret minimization, which is equivalent to return maximization in RL. Our analysis gives a theoretical explanation for some prioritization methods, including PER, LFIW and DisCor. Based on our theoretical analysis, we propose two practical prioritization strategies, ReMERN and ReMERT, that directly aims to improve the policy. ReMERN is robust to the randomness of environments, while ReMERT is more computational efficient and more accurate in environments with a stable temporal ordering of states. Our approaches obtain superior results compared to previous prioritized sampling methods. Future work can be conducted in the following two directions. First, the framework to obtain the optimal distribution in off-policy RL can be generalized to model-based RL and offline RL. Second, the two proposed algorithms are suitable for different kinds of MDP, so finding a unified prioritization method for all MDPs can further improve the performance.

Acknowledgements and Disclosure of Funding

We thank Xintong Qi and Xiaolong Yin for helpful discussions. We would also like to thank two groups of anonymous reviewers for their valuable comments on our paper. This work is supported by National Key Research and Development Program of China (2020AAA0107200) and NSFC(61876077).

References

- [1] Richard S Sutton and Andrew G Barto. *Reinforcement learning: An introduction*. MIT press, 2018.
- [2] Tuomas Haarnoja, Aurick Zhou, Pieter Abbeel, and Sergey Levine. Soft actor-critic: Off-policy maximum entropy deep reinforcement learning with a stochastic actor. In *Proceedings of the 35th International Conference on Machine Learning (ICML'18)*, pages 1856–1865, Stockholmsmässan, Sweden, 2018.
- [3] Scott Fujimoto, Herke van Hoof, and David Meger. Addressing function approximation error in actor-critic methods. In *Proceedings of the 35th International Conference on Machine Learning (ICML'18)*, pages 1582–1591, Stockholmsmässan, Sweden, 2018.
- [4] Matteo Hessel, Joseph Modayil, Hado van Hasselt, Tom Schaul, Georg Ostrovski, Will Dabney, Dan Horgan, Bilal Piot, Mohammad Gheshlaghi Azar, and David Silver. Rainbow: Combining improvements in deep reinforcement learning. In *Proceedings of the 32nd Conference on Artificial Intelligence (AAAI'18)*, pages 3215–3222, New Orleans, LA, 2018.
- [5] Volodymyr Mnih, Koray Kavukcuoglu, David Silver, Andrei A. Rusu, Joel Veness, Marc G. Bellemare, Alex Graves, Martin A. Riedmiller, Andreas Fidjeland, Georg Ostrovski, Stig Petersen, Charles Beattie, Amir Sadik, Ioannis Antonoglou, Helen King, Dharrshan Kumaran, Daan Wierstra, Shane Legg, and Demis Hassabis. Human-level control through deep reinforcement learning. *Nature*, 518(7540):529–533, 2015.
- [6] Marc G. Bellemare, Will Dabney, and Rémi Munos. A distributional perspective on reinforcement learning. In *Proceedings of the 34th International Conference on Machine Learning (ICML'17)*, pages 449–458, Sydney, Australia, 2017.
- [7] Long Ji Lin. Self-improving reactive agents based on reinforcement learning, planning and teaching. *Journal of Machine Learning Research*, 8:293–321, 1992.
- [8] Angelos Katharopoulos and François Fleuret. Not all samples are created equal: Deep learning with importance sampling. In *Proceedings of the 35th International Conference on Machine Learning (ICML'18)*, pages 2530–2539, Stockholmsmässan, Sweden, 2018.

- [9] Tom Schaul, John Quan, Ioannis Antonoglou, and David Silver. Prioritized experience replay. In *Proceedings of the 4th International Conference on Learning Representations (ICLR'16)*, San Juan, Puerto Rico, 2016.
- [10] Marc Brittain, Joshua R. Bertram, Xuxi Yang, and Peng Wei. Prioritized sequence experience replay. *CoRR*, abs/1905.12726, 2019.
- [11] Aviral Kumar, Abhishek Gupta, and Sergey Levine. Discor: Corrective feedback in reinforcement learning via distribution correction. In *Proceedings of 33rd conference on Neural Information Processing Systems (NeurIPS'20)*, virtual event, 2020.
- [12] Samarth Sinha, Jiaming Song, Animesh Garg, and Stefano Ermon. Experience replay with likelihood-free importance weights. *CoRR*, abs/2006.13169, 2020.
- [13] David Andre, Nir Friedman, and Ronald Parr. Generalized prioritized sweeping. In *proceedings of the 10th conference on Neural Information Processing Systems (NeurIPS'97)*, pages 1001–1007, Denver, CO, 1997.
- [14] Andrew W. Moore and Christopher G. Atkeson. Prioritized sweeping: Reinforcement learning with less data and less time. *Journal of Machine Learning Research*, 13:103–130, 1993.
- [15] Harm van Seijen and Richard S. Sutton. Planning by prioritized sweeping with small backups. In *Proceedings of the 30th International Conference on Machine Learning (ICML'13)*, pages 361–369, 2013.
- [16] Che Wang, Yanqiu Wu, Quan Vuong, and Keith Ross. Striving for simplicity and performance in off-policy DRL: output normalization and non-uniform sampling. In *Proceedings of the 37th International Conference on Machine Learning (ICML'20)*, pages 10070–10080, virtual event, 2020.
- [17] Kimin Lee, Michael Laskin, Aravind Srinivas, and Pieter Abbeel. SUNRISE: A simple unified framework for ensemble learning in deep reinforcement learning. In *Proceedings of the 38th International Conference on Machine Learning (ICML'21)*, pages 6131–6141, virtual event, 2021.
- [18] Justin Fu, Aviral Kumar, Matthew Soh, and Sergey Levine. Diagnosing bottlenecks in deep q-learning algorithms. In *Proceedings of the 36th International Conference on Machine Learning (ICML'19)*, pages 2021–2030, Long Beach, CA, 2019.
- [19] Scott Fujimoto, David Meger, and Doina Precup. An equivalence between loss functions and non-uniform sampling in experience replay. In *Proceedings of the 33rd Annual Conference on Neural Information Processing Systems (NeurIPS'20)*, 2020.
- [20] Shantong Zhang and Richard S. Sutton. A deeper look at experience replay. *CoRR*, abs/1712.01275, 2017.
- [21] William Fedus, Prajit Ramachandran, Rishabh Agarwal, Yoshua Bengio, Hugo Larochelle, Mark Rowland, and Will Dabney. Revisiting fundamentals of experience replay. In *Proceedings of the 37th International Conference on Machine Learning (ICML'20)*, pages 3061–3071, virtual event, 2020.
- [22] Scott Fujimoto, David Meger, and Doina Precup. Off-policy deep reinforcement learning without exploration. In *Proceedings of the 36th International Conference on Machine Learning (ICML'19)*, pages 2052–2062, Long Beach, CA, 2019.
- [23] Maxime Chevalier-Boisvert, Lucas Willems, and Suman Pal. Minimalistic gridworld environment for openai gym. <https://github.com/maximecb/gym-minigrid>, 2018.
- [24] Tianhe Yu, Deirdre Quillen, Zhanpeng He, Ryan Julian, Karol Hausman, Chelsea Finn, and Sergey Levine. Meta-world: A benchmark and evaluation for multi-task and meta reinforcement learning. In *Proceedings of the 3rd Conference on Robot Learning (CoRL'19)*, Osaka, Japan, 2019.

- [25] Emanuel Todorov, Tom Erez, and Yuval Tassa. Mujoco: A physics engine for model-based control. In *Proceedings of 24th International Conference on Intelligent Robots and Systems (IROS'12)*, pages 5026–5033, Vilamoura, Portugal, 2012.
- [26] Yuval Tassa, Saran Tunyasuvunakool, Alistair Muldal, Yotam Doron, Siqi Liu, Steven Bohez, Josh Merel, Tom Erez, Timothy Lillicrap, and Nicolas Heess. dm-control: Software and tasks for continuous control, 2020.
- [27] Jiayi Weng, Huayu Chen, Alexis Duburcq, Kaichao You, Minghao Zhang, Dong Yan, Hang Su, and Jun Zhu. Tianshou. <https://github.com/thu-ml/tianshou>, 2020.
- [28] Sham M. Kakade and John Langford. Approximately optimal approximate reinforcement learning. In *Proceedings of the 19th International Conference on Machine Learning (ICML'02)*, pages 267–274, Sydney, Australia, 2002.
- [29] Shi Dong, Benjamin Van Roy, and Zhengyuan Zhou. Provably efficient reinforcement learning with aggregated states. *CoRR*, abs/1912.06366, 2019.
- [30] Nan Jiang, Alex Kulesza, and Satinder P. Singh. Abstraction selection in model-based reinforcement learning. In *Proceedings of the 32nd International Conference on Machine Learning (ICML'15)*, pages 179–188, Lille, France, 2015.

A Proof of Theorem 3

In this section, we present detailed proofs for the theoretical derivation of Thm. 3, which aims to solve the following optimization problem:

$$\begin{aligned} \min_{w_k} \quad & \eta(\pi^*) - \eta(\pi_k) \\ \text{s.t.} \quad & Q_k = \arg \min_{Q \in \mathcal{Q}} \mathbb{E}_\mu[w_k(s, a) \cdot (Q - \mathcal{B}^* Q_{k-1})^2(s, a)], \\ & \mathbb{E}_\mu[w_k(s, a)] = 1, \quad w_k(s, a) \geq 0, \end{aligned} \quad (11)$$

The problem is equivalent to:

$$\begin{aligned} \min_{p_k} \quad & \eta(\pi^*) - \eta(\pi_k) \\ \text{s.t.} \quad & Q_k = \arg \min_{Q \in \mathcal{Q}} \mathbb{E}_{p_k}[(Q - \mathcal{B}^\pi Q_{k-1})^2(s, a)] \\ & \sum_{s, a} p_k(s, a) = 1, \quad p_k(s, a) \geq 0, \end{aligned} \quad (12)$$

The desired $w_k(s, a)$ is $\frac{p_k(s, a)}{\mu(s, a)}$, where $p_k(s, a)$ is the solution to the problem 12.

To solve Problem 12, we need to give the definition of *total variation distance*, *Wasserstein metric* and the diameter of a set, and introduce some mild assumptions.

Definition 3 (total variation distance). *The total variation (TV) distance of distribution P and Q is defined as*

$$D_{\text{TV}}(P, Q) = \frac{1}{2} \|P - Q\|_1$$

Definition 4 (Wasserstein metric). *For F, G two c.d.fs over the reals, the Wasserstein metric is defined as*

$$d_p(F, G) := \inf_{U, V} \|U - V\|_p$$

where the infimum is taken over all pairs of random variables (U, V) with respective cumulative distributions F and G.

Definition 5. *The diameter of a set A is defined as*

$$\text{diam}(A) = \sup_{x, y \in A} m(x, y)$$

where m is the metric on A.

Assumption 1. *The state space \mathcal{S} and action space \mathcal{A} are metric spaces with a metric m .*

Assumption 2. *The Q function is continuous with respect to $\mathcal{S} \times \mathcal{A}$.*

Assumption 3. *The transition function T is continuous with respect to $\mathcal{S} \times \mathcal{A}$ in the sense of Wasserstein metric, i.e.,*

$$\lim_{(s, a) \rightarrow (s_0, a_0)} d_p(T(\cdot | s, a), T(\cdot | s_0, a_0)) = 0,$$

where d_p denote the Wasserstein metric.

These assumptions are not strong and can be satisfied in most of environments includes MuJoCo, Atari games and so on.

Let $d_i^\pi(s)$ denote the discounted state distribution, where the state is visited by the agent for the i-th time. that is

$$d_i^\pi(s) = (1 - \gamma) \sum_{t_i=0}^{\infty} \gamma^{t_i} \Pr(s_{t_k} = s, \forall k \in [i]),$$

where $[k] = \{j \in \mathbb{N}_+ : j \leq k\}$. Notably,

$$d^\pi(s) = \sum_{i=1}^{\infty} d_i^\pi(s) \quad (13)$$

$$d_i^\pi(s) = \sum_{t=1}^{\infty} \rho^\pi(s, \pi(s), t) \gamma^t d_{i-1}^\pi(s), \quad (14)$$

where $\rho^\pi(s, \pi(s), t)$ is the shorthand for $\mathbb{E}_{a \sim \pi} \rho^\pi(s, a, t)$.

The standard definitions of Q function, value function and advantage function is:

$$\begin{aligned} Q^\pi(s, a) &= \mathbb{E}_\pi [\sum_{t \geq 0} \gamma^t r(s_t, a_t) | s_0 = s, a_0 = a]. \\ V^\pi(s) &= \mathbb{E}_\pi [\sum_{t \geq 0} \gamma^t r(s_t, a_t) | s_0 = s]. \\ A^\pi(s, a) &= Q^\pi(s, a) - V^\pi(s). \end{aligned}$$

In the follows, Lemma 1 is a technique used in Lemma 2. Lemma 2 shows that $\left| \frac{\partial d^\pi(s)}{\partial \pi(s)} \right|$ is a small quantity.

Lemma 1. Let f be an Lebesgue integrable function, P and Q are two probability distributions, $|f| \leq C$, then

$$|\mathbb{E}_{P(x)} f(x) - \mathbb{E}_{Q(x)} f(x)| \leq CD_{\text{TV}}(P, Q) \quad (15)$$

Proof.

$$\begin{aligned} |\mathbb{E}_{P(x)} f(x) - \mathbb{E}_{Q(x)} f(x)| &= \left| \sum_x [P(x)f(x) - Q(x)f(x)] \right| \\ &= \left| \sum_x [P(x)f(x) - Q(x)f(x)] \mathbb{I}[P(x) > Q(x)] \right. \\ &\quad \left. - \sum_x [P(x)f(x) - Q(x)f(x)] \mathbb{I}[P(x) < Q(x)] \right| \\ &\leq CD_{\text{TV}}(P, Q) \end{aligned}$$

□

Lemma 2. Let $\epsilon_\pi = \sup_{s,a} \sum_{t=1}^{\infty} \gamma^t \rho^\pi(s, a, t)$, we have

$$\left| \frac{\partial d^\pi(s)}{\partial \pi(s)} \right| \leq \epsilon_\pi d_1^\pi(s) \quad (16)$$

and $\epsilon_\pi \leq 1$.

Proof. The definition of $\rho^\pi(s, a, t)$ implies

$$0 \leq \sum_{t=1}^{\infty} \gamma^t \rho^\pi(s, a, t) \leq \epsilon_\pi \leq 1, \quad \forall a \in \mathcal{A}$$

Based on this fact, we have

$$\left| \sum_{t=1}^{\infty} \gamma^t (\rho^\pi(s, a_1, t) - \rho^\pi(s, a_2, t)) \right| \leq \epsilon_\pi, \quad \forall a_1, a_2 \in \mathcal{A}$$

Let $\rho^\pi(s, \pi(s), t)$ be a shorthand for $\mathbb{E}_{a \sim \pi(s)} \rho^\pi(s, a, t)$.

If π changes a little and becomes π' , and $\delta_a = D_{\text{TV}}(\pi(s), \pi'(s))$, then we have

$$\begin{aligned} & \left| \sum_{t=1}^{\infty} \gamma^t (\rho^\pi(s, \pi(s), t) - \rho^{\pi'}(s, \pi'(s), t)) \right| \\ &= \left| \mathbb{E}_{a_1 \sim \pi} \sum_{t=1}^{\infty} \gamma^t \rho^\pi(s, a_1, t) - \mathbb{E}_{a_2 \sim \pi'} \sum_{t=1}^{\infty} \gamma^t \rho^{\pi'}(s, a_1, t) \right| \\ &\leq \epsilon_\pi \delta_a \end{aligned} \tag{17}$$

This inequality comes from Lemma 1.

We denote the difference between $d_2^\pi(s)$ and $d_2^{\pi'}(s)$ as $\Delta d_2(s)$, which can be bounded as follows:

$$\begin{aligned} \Delta d_2(s) &= |d_2^\pi(s) - d_2^{\pi'}(s)| \\ &= \left| \sum_{t=1}^{\infty} \gamma^t (\rho^\pi(s, \pi(s), t) - \rho^{\pi'}(s, \pi'(s), t)) d_1^\pi(s) \right| \\ &= d_1^\pi(s) \left| \sum_{t=1}^{\infty} \gamma^t (\rho^\pi(s, \pi(s), t) - \rho^{\pi'}(s, \pi'(s), t)) \right| \\ &\leq \epsilon_\pi \delta_a d_1^\pi(s) \end{aligned}$$

Recursively, we have

$$\Delta d_i(s) \leq \epsilon_\pi^{i-1} \delta_a^{i-1} d_1^\pi(s)$$

Obviously, the change of π at state s won't change $d_1^\pi(s)$. According to Eq. (13),

$$\begin{aligned} \Delta d(s) &\leq \sum_{i=1}^{\infty} \Delta d_i(s) \\ &\leq \sum_{i=2}^{\infty} (\epsilon_\pi \delta_a)^{i-1} d_1^\pi(s) \\ &= \frac{\epsilon_\pi \delta_a}{1 - \epsilon_\pi \delta_a} d_1^\pi(s) \end{aligned}$$

According to $\frac{\partial d^\pi(s)}{\partial \pi(s)} = \lim_{\delta_a \rightarrow 0} \frac{\Delta d(s)}{\delta_a}$, we have

$$\left| \frac{\partial d^\pi(s)}{\partial \pi(s)} \right| \leq \epsilon_\pi d_1^\pi(s)$$

This concludes the proof. \square

Lemma 3. Given two policy π_1 and π_2 , where $\pi_1(a|s) = \frac{\exp(Q_1(s, a))}{\sum_{a'} \exp(Q_1(s, a'))}$. Then

$$\mathbb{E}_{a \sim \pi_2} Q_1(s, a) - \mathbb{E}_{a \sim \pi_1} Q_1(s, a) \leq 1$$

Proof. Suppose there are two actions a_1, a_2 under state s , and let $Q_1(s, a_1) = u, Q_1(s, a_2) = v$. Without loss of generality, let $u \leq v$.

$$\begin{aligned} \mathbb{E}_{a \sim \pi_2} Q_1(s, a) - \mathbb{E}_{a \sim \pi_1} Q_1(s, a) &\leq v - \frac{ue^u + ve^v}{e^u + e^v} \\ &= v - \frac{u + ve^{v-u}}{1 + e^{v-u}} \\ &= v - u - \frac{(v-u)e^{v-u}}{1 + e^{v-u}} \end{aligned}$$

Let $f(z) = z - \frac{ze^z}{1+e^z}$, the maximum point z_0 of $f(z)$ satisfies $f'(z_0) = 0$ where f' is the derivative of f , i.e., $\frac{e^{z_0}(1+z_0+e^{z_0})}{(1+e^{z_0})^2} - 1 = 0$. This implies $1 + e^{z_0} = z_0 e^{z_0}$ and $z_0 \in (1, 2)$. We have

$$\mathbb{E}_{a \sim \pi_2} Q_1(s, a) - \mathbb{E}_{a \sim \pi_1} Q_1(s, a) \leq f(v - u) \leq z_0 - 1 \leq 1$$

If the number of action is more than 2 and $Q_1(s, a_1) \geq Q_1(s, a_2) \geq \dots \geq Q_1(s, a_n)$, let b_1 represents a_1 and b_2 represents all other actions. Then $Q_1(s, b_1) = Q_1(s, a_1)$ and $Q_1(s, b_2) = \sum_{j=2}^n \frac{Q_1(s, a_j) \exp(Q_1(s, a_j))}{\sum_{k=2}^n \exp(Q_1(s, a_k))}$. In this way, we can derive the upper bound of $\mathbb{E}_{a \sim \pi_2} Q_1(s, a) - \mathbb{E}_{a \sim \pi_1} Q_1(s, a)$ as above. \square

The following lemma is proposed by Kakade,

Lemma 4 (Lemma 6.1 in [28]). *For any policy $\tilde{\pi}$ and π ,*

$$\eta(\tilde{\pi}) - \eta(\pi) = \frac{1}{1-\gamma} \mathbb{E}_{d^{\tilde{\pi}}(s,a)} [A_\pi(s,a)] \quad (18)$$

Lemma 5. *In discrete MDPs, let $\epsilon_{\pi_k} = \sup_{s,a} \sum_{t=1}^{\infty} \gamma^t \rho^{\pi_k}(s, a, t)$, the optimal solution p_k to a relaxation of optimization problem 12 satisfies the following relationship:*

$$p_k(s, a) = \frac{1}{Z^*} (D_k(s, a) + \epsilon_k(s, a)) \quad (19)$$

where $D_k(s, a) = d^{\pi_k}(s, a)(2 - \pi_k(a|s)) \exp(-|Q_k - Q^*(s, a)|) |Q_k - \mathcal{B}^* Q_{k-1}|(s, a)$, Z^* is the normalization constant and $\frac{\epsilon_k(s, a)}{D_k(s, a)} \leq \epsilon_{\pi_k}$.

Proof. Suppose $a^* \sim \pi^*(s)$. Let $\pi = \pi_k$, $\tilde{\pi} = \pi^*$ in Lemma 4, we have

$$\begin{aligned} & \eta(\pi^*) - \eta(\pi_k) \\ &= -\frac{1}{1-\gamma} \mathbb{E}_{d^{\pi_k}(s,a)} A_{\pi^*}(s,a) \\ &= \frac{1}{1-\gamma} \mathbb{E}_{d^{\pi_k}(s,a)} (V^*(s) - Q^*(s, a)) \\ &= \frac{1}{1-\gamma} \mathbb{E}_{d^{\pi_k}(s,a)} (V^*(s) - Q_k(s, a^*) + Q_k(s, a^*) - Q_k(s, a) + Q_k(s, a) - Q^*(s, a)) \quad (20) \\ &\stackrel{(a)}{\leq} \frac{1}{1-\gamma} \left(\mathbb{E}_{d^{\pi_k}(s)} (Q^*(s, a^*) - Q_k(s, a^*)) + \mathbb{E}_{d^{\pi_k}(s,a)} (Q_k(s, a) - Q^*(s, a)) + 1 \right) \\ &\leq \frac{1}{1-\gamma} \left(\mathbb{E}_{d^{\pi_k}(s)} |Q^*(s, a^*) - Q_k(s, a^*)| + \mathbb{E}_{d^{\pi_k}(s,a)} |Q_k(s, a) - Q^*(s, a)| + 1 \right) \\ &= \frac{2}{1-\gamma} \left(\mathbb{E}_{d^{\pi_k}, \pi^*} |Q_k(s, a) - Q^*(s, a)| + 1 \right), \end{aligned}$$

where $d^{\pi_k, \pi^*}(s, a) = d^{\pi_k}(s) \frac{\pi_k(a|s) + \pi^*(a|s)}{2}$ and (a) uses Lemma 3.

Since both sides of the above equation have the same minimum (here the minima are given by $Q_k = Q^*$), we can replace the objective in Problem 12 with the upper bound in Eq. (20) and solve the relaxed optimization problem.

$$\min_{p_k} \mathbb{E}_{d^{\pi_k}(s,a)} [|Q_k - Q^*|] \quad (21)$$

$$\text{s.t. } Q_k = \arg \min_{Q \in \mathcal{Q}} \mathbb{E}_{p_k} [(Q - \mathcal{B}^\pi Q_{k-1})^2(s, a)], \quad (22)$$

$$\sum_{s,a} p_k(s, a) = 1, \quad p_k(s, a) \geq 0. \quad (23)$$

Here we use $d^{\pi_k}(s, a)$ to replace d^{π_k, π^*} because we can not access π^* , and the best surrogate available is π_k .

Step 1: Jensen's Inequality. The optimization objective can be further relaxed with Jensen's Inequality, based on the fact that $f(x) = \exp(-x)$ is a convex function.

$$\mathbb{E}_{d^{\pi_k}(s,a)} [|Q_k - Q^*|] = -\log \exp(-\mathbb{E}_{d^{\pi_k}(s,a)} [|Q_k - Q^*|]) \leq -\log \mathbb{E}_{d^{\pi_k}(s,a)} [\exp(-|Q_k - Q^*|)] \quad (24)$$

Similarly, both sides of Eq. (24) have the same minimum. We obtain the following new optimization problem by replacing the objective with the upper bound in this equation:

$$\begin{aligned} & \min_{p_k} -\log \mathbb{E}_{d^{\pi_k}(s,a)}[\exp(-|Q_k - Q^*|)] \\ \text{s.t. } & Q_k = \arg \min_{Q \in \mathcal{Q}} \mathbb{E}_{p_k}[(Q - \mathcal{B}^* Q_{k-1})^2], \\ & \sum_{s,a} p_k(s,a) = 1, \quad p_k(s,a) \geq 0. \end{aligned} \tag{25}$$

Step 2: Computing the Lagrangian. In order to optimize problem 25, we follow the standard procedures of Lagrangian multiplier method. The Lagrangian is:

$$\mathcal{L}(p_k; \lambda, \mu) = -\log \mathbb{E}_{d^{\pi_k}(s,a)}[\exp(-|Q_k - Q^*|)] + \lambda(\sum_{s,a} p_k(s,a) - 1) - \mu^T p_k. \tag{26}$$

where λ and μ are the Lagrange multipliers.

Step 3: IFT gradient used in the Lagrangian. $\frac{\partial Q_k}{\partial p_k}$ can be computed according to implicit function theorem (IFT). The IFT gradient is given by:

$$\left. \frac{\partial Q_k}{\partial p_k} \right|_{Q_k, p_k} = -[\text{Diag}(p_k)]^{-1} [\text{Diag}(Q_k - \mathcal{B}^* Q_{k-1})] \tag{27}$$

The derivation is similar to that in [11].

Step 4: Approximation of the gradient used in the Lagrangian. We derive an expression for $\frac{\partial d^{\pi_k}(s,a)}{\partial p_k}$, which will be used when computing the gradient of the Lagrangian. We use π_k to denote the policy induced by Q_k .

$$\begin{aligned} \frac{\partial d^{\pi_k}(s,a)}{\partial p_k} &= \frac{\partial d^{\pi_k}(s,a)}{\partial \pi_k} \frac{\partial \pi_k}{\partial Q_k} \frac{\partial Q_k}{\partial p_k} \\ &= (d^{\pi_k}(s) + \epsilon_2(s)) \frac{\partial \pi_k}{\partial Q_k} \frac{\partial Q_k}{\partial p_k} \\ &\stackrel{(b)}{=} (d^{\pi_k}(s) + \epsilon_2(s)\pi_k(a|s)) \frac{\sum_{a' \neq a} \exp(Q_k(s,a'))}{\sum_{a'} \exp(Q_k(s,a'))} \frac{\partial Q_k}{\partial p_k} \\ &\stackrel{(c)}{=} d^{\pi_k}(s,a)(1 - \pi_k(a|s)) \frac{\partial Q_k}{\partial p_k} + \epsilon_2(s)\pi_k(a|s)(1 - \pi_k(a|s)) \frac{\partial Q_k}{\partial p_k} \end{aligned}$$

where $\epsilon_2(s) = \frac{\partial d^{\pi_k}(s)}{\partial \pi_k(s)}$. (b) and (c) are based on the fact that $\pi_k(a|s) = \frac{\exp(Q_k(s,a))}{\sum_{a'} \exp(Q_k(s,a'))}$.

Step 5: Computing optimal p_k . By KKT conditions, we have

$$\frac{\partial \mathcal{L}(p_k; \lambda, \mu)}{\partial p_k} = 0$$

$$\begin{aligned} & \frac{\partial \mathcal{L}(p_k; \lambda, \mu)}{\partial p_k} \\ &= \frac{\exp(-|Q_k - Q^*|(s,a))}{Z} (d^{\pi_k}(s,a) \text{sgn}(Q_k - Q^*) \cdot \frac{\partial Q_k}{\partial p_k} + \cdot \frac{\partial d^{\pi_k}(s,a)}{\partial p_k}) + \lambda - \mu_{s,a} \end{aligned}$$

where $Z = \mathbb{E}_{s',a' \sim d^{\pi_k}(s,a)} \exp(-|Q_k - Q^*|(s',a'))$. Substituting the expression of $\frac{\partial Q_k}{\partial p_k}$ and $\frac{\partial d^{\pi_k}(s,a)}{\partial p_k}$ with the results obtained in Step. 3 and Step. 4 respectively, and let $Z_{s,a} = Z(\lambda^* - \mu_{s,a}^*)$, we obtain

$$\begin{aligned} p_k(s,a) &= \left(d^{\pi_k}(s,a) (\text{sgn}(Q_k - Q^*) + 1 - \pi_k(a|s)) \exp(-|Q_k - Q^*|(s,a)) |Q_k - \mathcal{B}^* Q_{k-1}|(s,a) \right. \\ &\quad \left. + \epsilon_2(s)\pi_k(a|s)(1 - \pi_k(a|s)) \exp(-|Q_k - Q^*|(s,a)) |Q_k - \mathcal{B}^* Q_{k-1}|(s,a) \right) \frac{1}{Z_{s,a}} \end{aligned} \tag{28}$$

Notably, $Q_k \approx Q^{\pi_k} \leq Q^*$. Thus, $\text{sgn}(Q_k - Q^*)$ always is 1 approximately, so we can simplify this relationship as

$$p_k(s, a) = \frac{1}{Z_{s,a}} \left(d^{\pi_k}(s, a)(2 - \pi_k(a|s)) \exp(-|Q_k - Q^*|(s, a)) |Q_k - \mathcal{B}^* Q_{k-1}|(s, a) \right. \\ \left. + \epsilon_2(s)\pi_k(a|s)(1 - \pi_k(a|s)) \exp(-|Q_k - Q^*|(s, a)) |Q_k - \mathcal{B}^* Q_{k-1}|(s, a) \right) \quad (29)$$

The first term is always larger or equal to zero. The second term does not influence the sign of the equation because the absolute value of $\epsilon_2(s)$ is smaller than $d^{\pi_k}(s)$ according to Lemma 2. Note that Eq. (29) is always larger or equal to zero. If it is larger than zero then $\mu^* = 0$ by the KKT condition. If it is equal to zero, we can let $\mu^* = 0$ because the value of μ^* does not influence $w_k(s, a)$. Without loss of generality, we can let $\mu^* = 0$. Then $Z_{s,a} = Z^* = Z\lambda^*$ is a constant with respect to different s and a . In this way, we can simplify Eq. (29) as follows:

$$p_k(s, a) = \frac{1}{Z^*} (D_k(s, a) + \epsilon_k(s, a))$$

where $D_k(s, a) = d^{\pi_k}(s, a)(2 - \pi_k(a|s)) \exp(-|Q_k - Q^*|(s, a)) |Q_k - \mathcal{B}^* Q_{k-1}|(s, a)$ and $\epsilon_k(s, a) = \epsilon_2(s)\pi_k(a|s)(1 - \pi_k(a|s)) \exp(-|Q_k - Q^*|(s, a)) |Q_k - \mathcal{B}^* Q_{k-1}|(s, a)$.

Based on the expression of $D_k(s, a)$ and $\epsilon_k(s, a)$, we have

$$\frac{\epsilon_k(s, a)}{D_k(s, a)} = \frac{\epsilon_2(s)(1 - \pi_k(a|s))}{d^{\pi_k}(s)(2 - \pi_k(a|s))} \leq \epsilon_{\pi_k}$$

The inequality is from 2. This concludes the proof. \square

Theorem 3 (formal). Let $\epsilon_{\pi_k} = \sup_{s,a} \sum_{t=1}^{\infty} \gamma^t \rho^{\pi_k}(s, a, t)$. Under Assumption 1, 2 and 3, if $\frac{d^{\pi_k}(s,a)}{\mu(s,a)}$ exists, we have in MDPs with discrete action spaces, the solution w_k to the relaxed optimization problem 11 is

$$w_k(s, a) = \frac{1}{Z_1^*} (E_k(s, a) + \epsilon_{k,1}(s, a)). \quad (30)$$

In MDPs with continuous action spaces, the solution is

$$w_k(s, a) = \frac{1}{Z_2^*} (F_k(s, a) + \epsilon_{k,2}(s, a)). \quad (31)$$

where

$$E_k(s, a) = \frac{d^{\pi_k}(s, a)}{\mu(s, a)} (2 - \pi_k(a|s)) \exp(-|Q_k - Q^*|(s, a)) |Q_k - \mathcal{B}^* Q_{k-1}|(s, a)$$

$$F_k(s, a) = 2 \frac{d^{\pi_k}(s, a)}{\mu(s, a)} \exp(-|Q_k - Q^*|(s, a)) |Q_k - \mathcal{B}^* Q_{k-1}|(s, a),$$

Z_1^*, Z_2^* is the normalization constants and $\max \left\{ \frac{\epsilon_{k,1}(s,a)}{E_k(s,a)}, \frac{\epsilon_{k,2}(s,a)}{F_k(s,a)} \right\} \leq \epsilon_{\pi_k}$.

Proof. By Lemma 5, for MDPs with discrete action space and state space, we have

$$p_k(s, a) = \frac{1}{Z^*} (D_k(s, a) + \epsilon_k(s, a))$$

Based on the deviation of Problem 12, the solution in this situation is

$$w_k(s, a) = \frac{1}{Z^*} \left(\frac{D_k(s, a)}{\mu(s, a)} + \frac{\epsilon_k(s, a)}{\mu(s, a)} \right) \quad (32)$$

The existence of $\frac{d^{\pi_k}(s,a)}{\mu(s,a)}$ guarantees the existence of $\frac{D_k(s,a)}{\mu(s,a)}$ and $\frac{\epsilon_k(s,a)}{\mu(s,a)}$. Let $E_k(s, a) = \frac{D_k(s,a)}{\mu(s,a)}$ and $\epsilon_{k,1}(s, a) = \frac{\epsilon_k(s,a)}{\mu(s,a)}$, we get Eq. (30).

We derive the result for continuous action space and state space as follows, the result for continuous state space and discrete action space, and discrete state space and continuous action space can be derived similarly.

Remember that $\mathcal{B}^*Q_{k-1}(s, a) = r(s, a) + \gamma \max_{a'} \mathbb{E}_{s'} Q_{k-1}(s', a')$ and $Q_k(s, a) = \arg \min_Q (Q(s, a) - \mathcal{B}^*Q_{k-1}(s, a))^2$, if we use $R(s, a) = Q_k(s, a) - \gamma \max_{a'} \mathbb{E}_{s'} Q_{k-1}(s', a')$ to replace $r(s, a)$, then Q_k is still the desired Q function after the Bellman update. Since the continuity of Q_k , Q_{k-1} and T guarantee $R(s, a)$ is continuous, without loss of generality, we assume $r(s, a)$ is continuous.

We utilize the techniques in reinforcement learning with aggregated states [29]. Concretely, we can partition the set of all state-action pairs, with each cell representing an aggregated state. Such a partition can be defined by a function $\phi : \mathcal{S} \cup \mathcal{A} \mapsto \hat{\mathcal{S}} \cup \hat{\mathcal{A}}$, where $\hat{\mathcal{S}}$ is the space of aggregated states and $\hat{\mathcal{A}}$ is the space of aggregated actions. With such a partition, we can discretize the continuous spaces. For example, for the continuous space $\{x \in \mathbb{R} : 0 \leq x \leq 10\}$, define $\phi(x) = \sum_{i=1}^9 \mathbb{I}(x \leq x_i)$, and then the space of aggregated states becomes $\{0, 1, 2, \dots, 9\}$, which is a discrete space.

With function ϕ , we define the transition function and reward function in this new MDP. For all $\hat{s}, \hat{s}' \in \hat{\mathcal{S}}, \hat{a} \in \hat{\mathcal{A}}$

$$\begin{aligned}\hat{T}(\hat{s}'|\hat{s}, \hat{a}) &= \frac{\sum_{s,a \in \phi^{-1}(\hat{s}, \hat{a})} \mu(s, a) \sum_{s' \in \phi^{-1}(\hat{s}')} T(s'|s, a)}{\sum_{s,a \in \phi^{-1}(\hat{s}, \hat{a})} \mu(s, a)} \\ \hat{r}(\hat{s}, \hat{a}) &= \frac{\sum_{s,a \in \phi^{-1}(\hat{s}, \hat{a})} \mu(s, a) r(s, a)}{\sum_{s,a \in \phi^{-1}(\hat{s}, \hat{a})} \mu(s, a)}\end{aligned}\tag{33}$$

where $(\phi(s), \phi(a))$ is simplified as $\phi(s, a)$ and $\phi^{-1}(\hat{s}, \hat{a})$ is the preimage of (\hat{s}, \hat{a}) .

In this way, Eq. (32) holds for aggregated state space:

$$\hat{w}_k(\phi(s, a)) = \frac{1}{\hat{Z}^*} \left(\frac{\hat{D}_k(\phi(s, a))}{\hat{\mu}(\phi(s, a))} + \frac{\hat{\epsilon}_k(\phi(s, a))}{\hat{\mu}(\phi(s, a))} \right)\tag{34}$$

Suppose $\hat{\mathcal{S}}$ and $\hat{\mathcal{A}}$ is equipped with metric m' , we construct a sequence of functions ϕ_h , which satisfies

- (i) If $m(u_1 - u_2) \leq m(u_1 - u_3)$, then $m'(\phi_h(u_1) - \phi_h(u_2)) \leq m'(\phi_h(u_1) - \phi_h(u_3))$ for all $u_1, u_2, u_3 \in \mathcal{S}$ or $u_1, u_2, u_3 \in \mathcal{A}$.
- (ii) $\lim_{h \rightarrow \infty} \text{diam}(\phi_h^{-1}(c)) = 0$ for all $c \in \mathcal{S}' \cup \mathcal{A}'$.

Based on the two conditions on ϕ_h and the continuous of reward function and transition function, for all $s, s' \in \mathcal{S}$ and $a \in \mathcal{A}$,

$$\begin{aligned}\lim_{h \rightarrow \infty} |\hat{r}(\phi_h(s, a)) - r(s, a)| &= 0 \\ \lim_{h \rightarrow \infty} |\hat{T}(\phi_h(s')|\phi_h(s, a)) - T(s'|s, a)| &= 0\end{aligned}\tag{35}$$

This means the constructed MDP approaches the original MDP as h tends to infinity.

With the Lemma 3 in [30],

$$\begin{aligned}\lim_{h \rightarrow \infty} \mathcal{B}^*\hat{Q}_{k-1}(\phi_h(s, a)) &= \mathcal{B}^*Q_{k-1}(s, a) \\ \lim_{h \rightarrow \infty} \mathcal{B}^*\hat{Q}^*(\phi_h(s, a)) &= \mathcal{B}^*Q^*(s, a)\end{aligned}$$

Note that $Q_k(s, a) = \arg \min_Q (Q - \mathcal{B}^*Q_{k-1}(s, a))^2$, $\hat{Q}_k(\phi_h(s, a)) = \arg \min_Q (Q - \mathcal{B}^*\hat{Q}_{k-1}(\phi_h(s, a)))^2$, $Q^*(s, a) = \arg \min_Q (Q - \mathcal{B}^*Q^*(s, a))^2$ and $\hat{Q}^*(\phi_h(s, a)) = \arg \min_Q (Q - \mathcal{B}^*\hat{Q}^*(\phi_h(s, a)))^2$,

$$\begin{aligned}\lim_{h \rightarrow \infty} \hat{Q}_k(\phi_h(s, a)) &= Q_k(s, a) \\ \lim_{h \rightarrow \infty} \hat{Q}^*(\phi_h(s, a)) &= Q^*(s, a)\end{aligned}$$

Because $\pi(a|s) = \frac{\exp(Q(s,a))}{\sum_{a'} \exp(Q(s,a'))}$, π is continuous with respect to Q , then we have

$$\lim_{h \rightarrow \infty} \hat{\pi}_k(\phi_h(a)|\phi_h(s)) = \pi_k(a|s)$$

The continuity of π and transition function T guarantees

$$\lim_{h \rightarrow \infty} \hat{d}^{\hat{\pi}_k}(\phi_h(s, a)) = d^{\pi_k}(s, a)$$

Therefore,

$$\begin{aligned} \lim_{h \rightarrow \infty} |\hat{Q}_k - \hat{Q}^*|(\phi((s, a))) &= |Q_k - Q^*|(s, a) \\ \lim_{h \rightarrow \infty} |\hat{Q}_k - \hat{\mathcal{B}}^* \hat{Q}^*|(\phi((s, a))) &= |Q_k - \mathcal{B}^* Q_{k-1}|(s, a) \\ \lim_{h \rightarrow \infty} \frac{d^{\hat{\pi}_k}(\phi_h(s, a))}{\hat{\mu}(\phi_h(s, a))} &= \frac{d^{\pi_k}(s, a)}{\mu(s, a)} \end{aligned} \quad (36)$$

Notably, $\epsilon_2(s)\pi_k(a|s) \leq d^{\pi_k}(s, a)$, the existence of $\frac{d^{\pi_k}(s, a)}{\mu(s, a)}$ implies the existence of $\frac{\epsilon_2(s)\pi_k(a|s)}{\mu(s, a)}$.

$$\lim_{h \rightarrow \infty} \frac{\hat{\epsilon}_k(\phi(s, a))}{\hat{\mu}(\phi(s, a))} = \epsilon_{k,1}(s, a) \quad (37)$$

where $\epsilon_{k,1} = \frac{\epsilon_k(s)\pi_k(a|s)}{\mu(s, a)}(1 - \pi_k(a|s)) \exp(-|Q_k - Q^*|(s, a)) |Q_k - \mathcal{B}^* Q_{k-1}|(s, a)$.

Using the Eq. (A), (36) and (37), we have

$$w_k(s, a) = \frac{1}{Z_1^*} (E_k(s, a) + \epsilon_{k,1}(s, a)).$$

If the action space is continuous, $\pi_k(a|s) = 0$, then we have

$$w_k(s, a) = \frac{1}{Z_2^*} (F_k(s, a) + \epsilon_{k,2}(s, a))$$

The upper bound of $\frac{\epsilon_{k,1}(s, a)}{E_k(s, a)}$ and $\frac{\epsilon_{k,2}(s, a)}{F_k(s, a)}$ can be derived directly from Lemma 5. This concludes our proof. \square

B Detailed Proof of Theorem 2

Let $(\mathcal{B}Q)_k(s, a)$ denote $|Q_k(s, a) - \mathcal{B}^* Q_k(s, a)|$. We first introduce an assumption.

Assumption 4. At iteration k , $(\mathcal{B}Q)_k(s, a)$ is independent of $(\mathcal{B}Q)_k(s', a')$ if $(s, a) \neq (s', a')$ for all $k > 0$.

This assumption is not strong. If we use a table to represent Q function, it holds apparently. Notably, though we need this assumption in our proof, we can also apply our method on the situation where this assumption doesn't hold. With this assumption, we have the following theorem.

Lemma 6. Consider a MDP, trajectories $\tau_i = \{s_t^i, a_t^i\}_{t=0}^{T_i}, i = 0, 1, \dots$ is generated by a policy π under this MDP, then we have

$$\begin{aligned} |Q_k(s, a) - Q^*(s, a)| &\leq |Q_k(s_t, a_t) - \mathcal{B}^* Q_{k-1}(s_t, a_t)| \\ &\quad + \mathbb{E}_\tau \left(\sum_{t'=1}^{h_\tau^{\pi_k}(s, a)} \gamma^{t'} \left((\mathcal{B}Q)_{k-1}(s_{t'}, a_{t'}) + c \right) + \gamma^{h_\tau^{\pi_k}(s, a)+1} c \right) \end{aligned} \quad (38)$$

where $(\mathcal{B}Q)_k(s_{h_\tau^{\pi_k}(s, a)}, a_{h_\tau^{\pi_k}(s, a)}) = |Q_k(s_{h_\tau^{\pi_k}(s, a)}, a_{h_\tau^{\pi_k}(s, a)}) - r(s_{h_\tau^{\pi_k}(s, a)}, a_{h_\tau^{\pi_k}(s, a)})|$, $c = \max_{s,a} (Q^*(s, a^*) - Q^*(s, a))$, and $(s_{t'}, a_{t'})$ is the t' -th state-action pair behind (s, a) .

Proof.

$$\begin{aligned}
& |Q_k(s_t, a_t) - Q^*(s_t, a_t)| \\
&= |Q_k(s_t, a_t) - \mathcal{B}^*Q_{k-1}(s_t, a_t) + \mathcal{B}^*Q_{k-1}(s_t, a_t) - \mathcal{B}^*Q^*(s_t, a_t)| \\
&\stackrel{(a)}{\leq} |Q_k(s_t, a_t) - \mathcal{B}^*Q_{k-1}(s_t, a_t)| \\
&\quad + \gamma |\mathbb{E}_{p(\tau)}[Q_{k-1}(s_{t+1}, a_{t+1}) - Q^*(s_{t+1}, a_{t+1}) + Q^*(s_{t+1}, a_{t+1}) - Q^*(s_{t+1}, a^*)]| \\
&\stackrel{(b)}{\leq} |Q_k(s_t, a_t) - \mathcal{B}^*Q_{k-1}(s_t, a_t)| + \gamma c + \gamma \mathbb{E}_\tau [|Q_{k-1}(s_{t+1}, a_{t+1}) - Q^*(s_{t+1}, a_{t+1})|]
\end{aligned}$$

where the expectation is taken over $s' \sim P(s'|s, a)$, $a' \sim \pi(a'|s')$. (a) uses triangle inequality, (b) is because $f(x) = |x|$ is convex function and using Jensen's Inequality.

Similarly, we have

$$\begin{aligned}
& |Q_{k-1}(s_{t+1}, a_{t+1}) - Q^*(s_{t+1}, a_{t+1})| \\
&= |Q_{k-1}(s_{t+1}, a_{t+1}) - \mathcal{B}^*Q_{k-1}(s_{t+1}, a_{t+1}) + \mathcal{B}^*Q_{k-1}(s_{t+1}, a_{t+1}) - \mathcal{B}^*Q^*(s_{t+1}, a_{t+1})| \\
&\leq (\mathcal{B}Q)_{k-1}(s_{t+1}, a_{t+1}) + \gamma c + \gamma \mathbb{E}_\tau [|Q_{k-1}(s_{t+2}, a_{t+2}) - Q^*(s_{t+2}, a_{t+2})|]
\end{aligned}$$

Recursively,

$$\begin{aligned}
& |Q_k(s, a) - Q^*(s, a)| \\
&\leq |Q_k(s_t, a_t) - \mathcal{B}^*Q_{k-1}(s_t, a_t)| + \sum_{t'=1}^{h_\tau^{\pi_k}(s, a)} \gamma^{t'} \left((\mathcal{B}Q)_{k-1}(s_{t'}, a_{t'}) + c \right) + \gamma^{h_\tau^{\pi_k}(s, a)+1} c \quad (39)
\end{aligned}$$

where $(\mathcal{B}Q)_{k-1}(s_{h_\tau^{\pi_k}(s, a)}, a_{h_\tau^{\pi_k}(s, a)}) = |Q_{k-1}(s_{h_\tau^{\pi_k}(s, a)}, a_{h_\tau^{\pi_k}(s, a)}) - r(s_{h_\tau^{\pi_k}(s, a)}, a_{h_\tau^{\pi_k}(s, a)})|$. \square

This theorem shows that the cumulative Bellman error with a constant c is an upper bound of $|Q_k - Q^*|$, so we can use Bellman error with the constant to estimate this quantity.

Suppose the Q function is equipped with a learning rate α , i.e., $Q_k = \alpha(\mathcal{B}^*Q_{k-1} - Q_{k-1}) + (1 - \alpha)Q_{k-1}$, we have the following lemma,

Lemma 7.

$$\begin{aligned}
\|\mathcal{B}^*Q_k - Q_k\|_\infty &\leq (\alpha\gamma + 1 - \alpha)^k \|\mathcal{B}^*Q_0 - Q_0\|_\infty \\
\|\mathcal{B}^*Q_{k-1} - Q_k\|_\infty &\leq (1 - \alpha)(\alpha\gamma + 1 - \alpha)^{k-1} \|\mathcal{B}^*Q_0 - Q_0\|_\infty \quad (40)
\end{aligned}$$

Proof.

$$\begin{aligned}
Q_k &= Q_{k-1} + \alpha(\mathcal{B}^*Q_{k-1} - Q_{k-1}) \\
\implies \mathcal{B}^*Q_{k-1} - Q_k &= \frac{1 - \alpha}{\alpha} (Q_k - Q_{k-1})
\end{aligned}$$

$$\begin{aligned}
\|\mathcal{B}^*Q_k - Q_k\|_\infty &\leq \|\mathcal{B}^*Q_k - \mathcal{B}^*Q_{k-1}\|_\infty + \|\mathcal{B}^*Q_{k-1} - Q_k\|_\infty \\
&\leq \gamma \|Q_k - Q_{k-1}\|_\infty + \|\mathcal{B}^*Q_{k-1} - Q_k\|_\infty \\
&\leq \left(\gamma + \frac{1 - \alpha}{\alpha} \right) \|Q_k - Q_{k-1}\|_\infty \quad (41) \\
&\leq (\alpha\gamma + 1 - \alpha) \|\mathcal{B}^*Q_{k-1} - Q_{k-1}\|_\infty
\end{aligned}$$

$$\begin{aligned}
\|Q_k - \mathcal{B}^*Q_{k-1}\|_\infty &\leq (1 - \alpha) \|Q_{k-1} - \mathcal{B}^*Q_{k-1}\|_\infty \\
&\leq (1 - \alpha) (\|Q_{k-1} - \mathcal{B}^*Q_{k-2}\|_\infty + \|\mathcal{B}^*Q_{k-2} - \mathcal{B}^*Q_{k-1}\|_\infty) \\
&\leq (1 - \alpha) (\gamma \|Q_{k-2} - Q_{k-1}\|_\infty + \|Q_{k-1} - \mathcal{B}^*Q_{k-2}\|_\infty) \quad (42) \\
&\stackrel{(a)}{\leq} (1 - \alpha) \left(\gamma + \frac{1 - \alpha}{\alpha} \right) \|Q_{k-1} - Q_{k-2}\|_\infty \\
&\leq (1 - \alpha) (\alpha\gamma + 1 - \alpha) \|\mathcal{B}^*Q_{k-2} - Q_{k-2}\|_\infty
\end{aligned}$$

Then we can finish the proof by recursively applying Eq. (41) and (42). \square

Lemma 8 (Azuma). *Let X_0, X_1, \dots be a martingale such that, for all $k \geq 1$, $|X_k - X_{k-1}| \leq c_k$. Then*

$$\Pr[|X_n - X_0| \geq t] \leq 2 \exp\left(-\frac{t^2}{2 \sum_{k=1}^n c_k^2}\right). \quad (43)$$

In the follows, we denote $\sum_{t=1}^{h_\tau^{\pi_k}(s,a)} \gamma^t (\mathcal{B}Q)_k(s_t, a_t)$ as $\mathcal{B}(s, a, k)$.

Lemma 9. *Let $\phi_k = (\alpha\gamma + 1 - \alpha)^k \|\mathcal{B}^* Q_0 - Q_0\|_\infty$, $f(t) = \frac{\gamma - \gamma^{t+1}}{1-\gamma}$ and $\epsilon_{\pi_k} = \sup_{s,a} \sum_{t=1}^{\infty} \gamma^t \rho^{\pi_k}(s, a, t)$. Under Assumption 4, with probability at least $1 - \delta$,*

$$|\mathcal{B}(s, a, k) - f(h_\tau^{\pi_k}(s, a)) \mathbb{E}[(\mathcal{B}Q)_k(s_t, a_t)]| \leq \sqrt{2f(h_\tau^{\pi_k}(s, a))^2 (1 + \epsilon_{\pi_k})^2 \phi_k^2 \log \frac{2}{\delta}}. \quad (44)$$

Proof. Let $\mathcal{F}_h = \sigma_t(s_0, a_0, r_0, \dots, s_{h-1}, a_{h-1}, r_{h-1})$ be the σ -field summarising the information available just before s_t is observed.

Define $Y_h = \mathbb{E}[\mathcal{B}(s, a, k) | \mathcal{F}_h]$, then Y_h is a martingale because

$$\mathbb{E}[Y_h | \mathcal{F}_{h-1}] = \mathbb{E}[\mathbb{E}[\mathcal{B}(s, a, k) | \mathcal{F}_h] | \mathcal{F}_{h-1}] = \mathbb{E}[\mathcal{B}(s, a, k) | \mathcal{F}_{h-1}] = Y_{h-1}$$

$$\begin{aligned} |Y_h - Y_{h-1}| &\leq \gamma^h (1 + \epsilon_{\pi_k}) \|\mathcal{B}^* Q_k - Q_k\|_\infty \\ &\leq \gamma^h (1 + \epsilon_{\pi_k}) (\alpha\gamma + 1 - \alpha)^k \|\mathcal{B}^* Q_0 - Q_0\|_\infty = \gamma^h (1 + \epsilon_{\pi_k}) \phi_k \end{aligned}$$

By Azuma's lemma,

$$\Pr\left(|\mathcal{B}(s, a, k) - \mathbb{E}[\mathcal{B}(s, a, k)]| \geq \sqrt{2 \left(\frac{\gamma - \gamma^{h_\tau^{\pi_k}+1}}{1-\gamma}\right)^2 (1 + \epsilon_{\pi_k})^2 \phi_k^2 \log \frac{2}{\delta}}\right) \leq \delta$$

□

Since $(\alpha\gamma + 1 - \alpha)$ is less than 1, ϕ_k decreases exponentially as k increases. This theorem shows that we can use the average Bellman error as a surrogate of Bellman error at specific state-action pair without losing too much accuracy. In this way, $|Q_k - Q^*(s, a)|$ is merely related to the distance to end of the state-action pair.

Theorem 4 (formal). *Under Assumption 4, with probability at least $1 - \delta$, we have*

$$\begin{aligned} &|Q_k(s, a) - Q^*(s, a)| \\ &\leq \mathbb{E}_\tau \left(f(h_\tau^{\pi_k}(s, a)) (\mathbb{E}[(\mathcal{B}Q)_k(s_{t'}, a_{t'})] + c) + \gamma^{h_\tau^{\pi_k}(s,a)+1} c \right) + g(k, \delta) \end{aligned} \quad (45)$$

where $g(k, \delta) = (1 - \alpha)\phi_{k-1} + \sqrt{2f(h_\tau^{\pi_k}(s, a))^2 (1 + \epsilon_{\pi_k})^2 \phi_k^2 \log \frac{2}{\delta}}$.

Proof. According to Lemma 6, we have

$$\begin{aligned} |Q_k(s, a) - Q^*(s, a)| &\leq |Q_k(s_t, a_t) - \mathcal{B}^* Q_{k-1}(s_t, a_t)| \\ &\quad + \mathbb{E}_\tau \left(\sum_{t'=1}^{h_\tau^{\pi_k}(s,a)} \gamma^{t'} \left((\mathcal{B}Q)_{k-1}(s_{t'}, a_{t'}) + c \right) + \gamma^{h_\tau^{\pi_k}(s,a)+1} c \right) \end{aligned} \quad (46)$$

Using Lemma 7, we can upper bound $|Q_k(s_t, a_t) - \mathcal{B}^* Q_{k-1}(s_t, a_t)|$ as $(1 - \alpha)\phi_{k-1}$. With Lemma 9, $\sum_{t=1}^{h_\tau^{\pi_k}(s,a)} \gamma^t (\mathcal{B}Q)_k(s_t, a_t)$ can be bounded by right hand side of Eq. (44) with probability $1 - \delta$.

Substitute the bounds into Eq. (46), we have

$$\begin{aligned}
|Q_k(s, a) - Q^*(s, a)| &\leq (1 - \alpha)\phi_{k-1} + \sqrt{2f(h_\tau^{\pi_k}(s, a))^2(1 + \epsilon_{\pi_k})^2\phi_k^2 \log \frac{2}{\delta}} \\
&\quad + \mathbb{E}_\tau \left(f(h_\tau^{\pi_k}(s, a))(\mathbb{E}[(\mathcal{B}Q)_k(s_{t'}, a_{t'})] + c) + \gamma^{h_\tau^{\pi_k}(s, a)+1}c \right) \\
&\leq g(k, \delta) \\
&\quad + \mathbb{E}_\tau \left(f(h_\tau^{\pi_k}(s, a))(\mathbb{E}[(\mathcal{B}Q)_k(s_{t'}, a_{t'})] + c) + \gamma^{h_\tau^{\pi_k}(s, a)+1}c \right)
\end{aligned}$$

□

C Algorithms

Algorithm 1 ReMERN

- 1: Initialize Q-values $Q_\theta(s, a)$, a replay buffer μ , an **error model** $\Delta_\phi(s, a)$, and a **weight model** κ_ψ .
- 2: **for** step k in $\{1, \dots, N\}$ **do**
- 3: Collect M samples using π_k , add them to replay buffer μ , sample $\{(s_i, a_i)\}_{i=1}^N \sim \mu$.
- 4: Evaluate $Q_\theta(s, a)$, $\Delta_\phi(s, a)$ and $\kappa_\psi(s, a)$ on samples (s_i, a_i) .
- 5: Compute target values for Q and Δ on samples:
 $y_i = r_i + \gamma \max_{a'} Q_{k-1}(s'_i, a')$.
 $\hat{a}_i = \arg \max_a Q_{k-1}(s'_i, a)$.
 $\hat{\Delta} = |Q_\theta(s, a) - y_i| + \gamma \Delta_{k-1}(s'_i, \hat{a}_i)$.
- 6: **Optimize** κ_ψ using

$$L_\kappa(\psi) := \mathbb{E}_{\mathcal{D}_s} [f^*(f'(\kappa_\psi(s, a)))] - \mathbb{E}_{\mathcal{D}_f} [f'(\kappa_\psi(s, a))].$$

- 7: **Compute** w_k using

$$w_k(s, a) \propto \frac{d^{\pi_k}(s, a)}{\mu(s, a)} \exp \left(-\gamma \left[P^{\pi^{w_{k-1}}} \Delta_{k-1} \right] (s, a) \right).$$

- 8: Minimize Bellman error for Q_θ weighted by w_k .
 $\theta_{k+1} \leftarrow \operatorname{argmin}_\theta \frac{1}{N} \sum_i^N w_k(s_i, a_i) (Q_\theta(s_i, a_i) - y_i)^2$.
 - 9: Minimize ADP error for training ϕ .
 $\phi_{k+1} \leftarrow \operatorname{argmin}_\phi \frac{1}{N} \sum_{i=1}^N (\Delta_\phi(s_i, a_i) - \hat{\Delta}_i)^2$.
 - 10: **end for**
-

Algorithm 2 ReMERT

- 1: Initialize Q-values $Q_\theta(s, a)$, a replay buffer μ , and a weight model κ_ψ .
 - 2: **for** step k in $\{1, \dots, N\}$ **do**
 - 3: Collect M samples using π_k , add them to replay buffer μ , sample $\{(s_i, a_i)\}_{i=1}^N \sim \mu$.
 - 4: Evaluate $Q_\theta(s, a)$ and $\kappa_\psi(s, a)$ on samples (s_i, a_i) .
 - 5: Compute target values for Q on samples:
 $y_i = r_i + \gamma \max_{a'} Q_{k-1}(s'_i, a')$.
 $\hat{a}_i = \arg \max_a Q_{k-1}(s'_i, a)$.
 - 6: **Optimize** κ_ψ **using**

$$L_\kappa(\psi) := \mathbb{E}_{\mathcal{D}_s} [f^*(f'(\kappa_\psi(s, a)))] - \mathbb{E}_{\mathcal{D}_t} [f'(\kappa_\psi(s, a))]$$
.
 - 7: **Compute** w_k **using**

$$w_k(s, a) \propto \frac{d^{\pi_k}(s, a)}{\mu(s, a)} \exp \left(-\mathbb{E}_{q_{k-1}(\tau)} \text{TCE}_c(s, a) \right).$$
 - 8: Minimize Bellman error for Q_θ weighted by w_k .

$$\theta_{k+1} \leftarrow \operatorname{argmin}_\theta \frac{1}{N} \sum_i^N w_k(s_i, a_i) (Q_\theta(s_i, a_i) - y_i)^2.$$
 - 9: **end for**
-

D Experiments

We now present some additional experimental results and experiment details which we could not present due to shortage of space in the main body.

D.1 Cumulative Recurring Probability on Atari Games

Table 2: The value of ϵ_π with different policies in Atari games.

	Initial (Random) policy	Policy at timestep 100k	Policy at timestep 200k
Pong	0.00	0.00	0.00
Breakout	0.00	0.00	0.00
Kangaroo	0.44	0.32	0.15
KungFuMaster	0.66	0.06	0.01
MsPacman	0.44	0.04	0.00
Qbert	0.02	0.05	0.00
Enduro	0.00	0.00	0.00

In Pong, Breakout and Enduro, ϵ_π keeps zero, so there is no error terms in such environments. For KungFuMaster and MsPacman, though ϵ_π is high for the initial policy, its value decreases rapidly as the policy updates. The error term in Kangaroo induces some error but ϵ_π is still much smaller than one. The experiment results imply we can ignore the error term in most reinforcement learning environments.

D.2 Illustrations on Stable Temporal Structure

We conduct an extra experiment in the GridWorld environment to support our claim that the trajectories have a stable temporal ordering of states. Fig. 7 shows an empirical verification of the stable temporal ordering of states property.

The result shows that the variance of distance to end in one state is not large and decreases fast in training process. This means the property is not a strong assumption and can be satisfied in many environments.

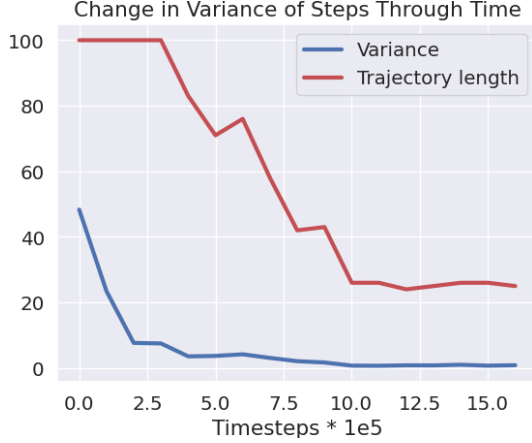


Figure 7: Change in variance of distance to end through time. For each timestep, the red line shows the average trajectory length in the last 500 states. The blue line shows the average variance of the last 500 states, where the variance for each state is calculated from its positions in their corresponding trajectories.

D.3 Description of Involved Environments

The Meta-World benchmark [24] includes a series of robotic manipulation tasks. These tasks differ from traditional goal-based ones in that the target objects of the robot. For example, the screw in the hammer task has randomized positions and can not be observed by RL agents. Therefore, Meta-World suite can be highly challenging for current state-of-the-art off policy RL algorithms. Visual descriptions for the Meta-World tasks are shown in Fig. 8. DisCor [11] showed preferable performance on some Meta-World tasks compared to SAC and PER [9], but the learning process is slow and unstable.

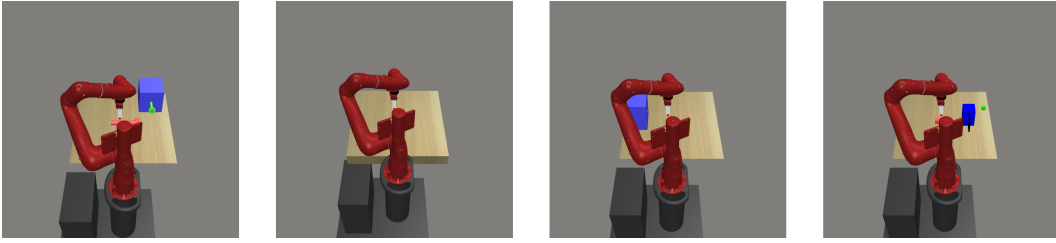


Figure 8: Pictures for Meta-World tasks hammer, sweep, peg-insert-side and stick-push.

D.4 Extended Results on Atari Environment

We evaluate ReMERN on an extended collection of Atari environments. As is shown in Tab. 3, ReMERN outperforms baseline methods in most of the environments.

D.5 Extended Evaluation on Gridworld

Aside from the FourRooms environment in Gridworld, we also conduct comparative evaluation on the Maze environment. The results are shown in Fig. 9. The Maze environment perfectly fits for our TCE-based prioritization, and TCE achieves the best performance among other methods.

D.6 The Relation Between Distance to End and $|Q_k - Q^*|$

In section D.5, the relationship between $|Q_k - Q^*|$ and distance to end has been shown in tabular environments. In this section, we explore the relationship in environments with continuous state and

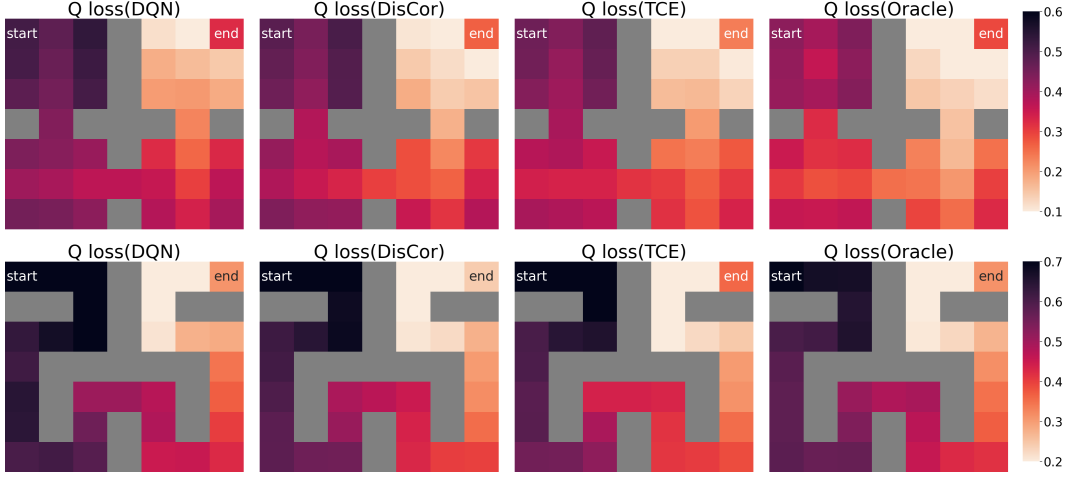


Figure 9: Extended evaluation results on Gridworld.

action spaces, i.e., Ant and Hopper tasks of MuJoCo environment. Since Q^* is inaccessible in these complex continuous control tasks, we approximate it by doing Monte-Carlo rollout using the best policy during training. The results are shown in Fig. 10.

The negative correlation between the two quantities is obvious in Ant-v2, but vague in Hopper-v2. It is because Hopper is a relatively easy task so that all state-action pair have small Q loss and don't have such correlation. The performance of ReMERT shown in Section 4 accords with this observation. ReMERT outperforms other algorithms in environments with a high correlation between the two quantities, and has a relatively poor performance in environments without such correlation.

D.7 Implementation Details

D.7.1 Algorithm Details

Weight Normalization To stabilize the prioritization, we apply normalization to the estimation of two terms: $\frac{d\pi_k(s,a)}{\mu(s,a)}$ and $\exp(-|Q_k - Q^*|)$.

Table 3: Extended experiments on Atari.

Environments	DQN(Nature)	DQN(Baseline)	PER(rank-b.)	ReMERT(Ours)
Assault	3395 ± 775	8260 ± 2274	3081	9952 ± 3249
BankHeist	429 ± 650	1116 ± 34	824	1166 ± 82
BeamRider	6846 ± 1619	5410 ± 1178	12042	5542 ± 1577
Breakout	401 ± 27	242 ± 79	481	223 ± 79
Enduro	302 ± 25	1185 ± 100	1266	1303 ± 258
Kangaroo	6740 ± 2959	6210 ± 1007	9053	7572 ± 1794
KungFuMaster	23270 ± 5955	29147 ± 7280	20181	35544 ± 8432
MsPacman	2311 ± 525	3318 ± 647	964.7	3481 ± 1350
Riverraid	8316 ± 1049	9609 ± 1293	10205	10215 ± 1815
SpaceInvaders	1976 ± 893	925 ± 371	1697	877 ± 249
UpNDown	8456 ± 3162	134502 ± 68727	16627	145235 ± 94643
Qbert	10596 ± 3294	13437 ± 2537	12741	14511 ± 1138
Zaxxon	4977 ± 1235	5070 ± 997	5901	5738 ± 1296

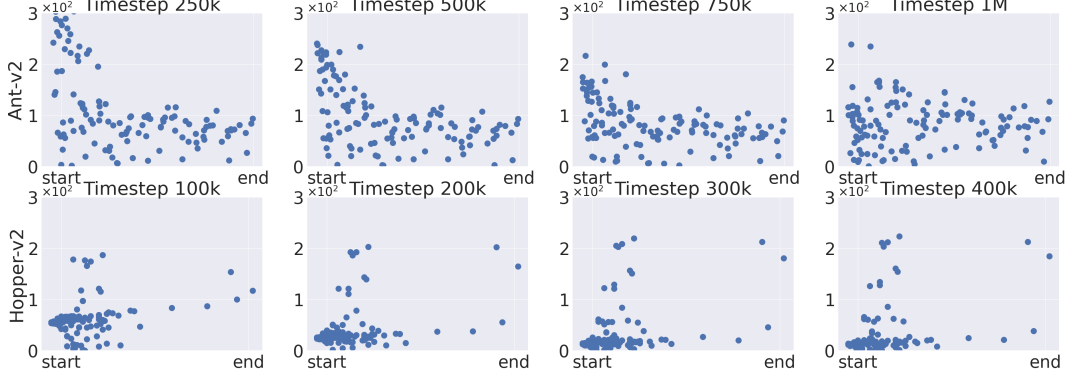


Figure 10: The relationship between $|Q_k - Q^*|$ and distance to end in two MuJoCo tasks (Ant and Hopper).

First, we introduce the normalization in calculating $\frac{d^{\pi_k}(s,a)}{\mu(s,a)}$, which aims to address the finite sample size issue. The normalization is:

$$\tilde{\kappa}_\psi(s, a) := \frac{\kappa_\psi(s, a)^{1/T}}{\mathbb{E}_{\mathcal{D}_s}[\kappa_\psi(s, a)^{1/T}]}$$

where \mathcal{D}_s is the slow buffer and T is temperature.

ReMERN uses Δ_ϕ to fit the discounted cumulative Bellman error. However, the Bellman error has different scales in various environments, leading to erroneous weight. We normalize it by dividing a moving average of Bellman error. The divisor is denoted as τ . Then the estimation of $\exp(-|Q_k - Q^*|)$ becomes

$$\exp\left(-\frac{\gamma [P^{\pi^{w_{k-1}}} \Delta_{k-1}](s, a)}{\tau}\right)$$

Truncated TCE TCE may suffer from a big deviation when $h_\tau^\pi(s, a)$ is too large or too small. To tackle this issue and improve the stability of the prioritization, we clip the output of TCE into $[b_1, b_2]$, where b_1 and b_2 are regarded as hyperparameters.

Baselines For the ReMERN and ReMERT algorithms in continuous action spaces with sensory observation, we alter the re-weighting strategy to $\frac{d^{\pi_k}(s,a)}{\mu(s,a)}$ and TCE approximation based on the source code provided by DisCor⁴. For the algorithms in discrete action spaces with pixel observation, we employ the baseline Tianshou⁵ [27] and add corresponding components.

D.7.2 Hyperparameter Details

The hyperparameters of our ReMERN and ReMERT algorithms include network architectures, learning rates, temperatures in on-policy reweight and DisCor, and the lower and upper bound in TCE algorithm. They are specified as follows:

- **Network architectures** We use standard Q and policy network in MuJoCo benchmark with hidden network sizes [256, 256]. In Meta-World we add an extra layer and the hidden network sizes are [256, 256, 256]. The networks computing Δ and κ have one extra layer than the corresponding Q and policy network.
- **Learning rates** The learning rate for continuous control tasks, including Meta-World, MuJoCo and DMC, is set to be 3e-4 for Q and policy networks alike. For Atari games, the learning rate is set to be 1e-4 and fixed across all environments.

⁴<https://github.com/ku2482/discor.pytorch>

⁵<https://github.com/thu-ml/tianshou>

- **Temperatures** The temperature for weights related with $\frac{d^{\pi_k}(s,a)}{\mu(s,a)}$ is 7.5 and fixed across different environments. Also, DisCor has a temperature hyperparameter related to the output normalization of the error network. We keep it unchanged in the Meta-World and DMC benchmark, and divide it by 20 in MuJoCo environments to make it compatible with on-policy prioritization weights.
- **Bounds in TCE** We select time-adaptive lower and upper bounds for TCE. The lower bound rises from 0.4 when training begins to 0.9 when it ends, and the upper bound drops from 1.6 to 1.1 accordingly. The bounds are fixed across different environments.
- **Random Seeds** In MuJoCo, Meta-World and DMC benchmarks, we run each experiment with four random seeds. The results are plotted with the mean of the four experiments. In Atari games, we run experiments with three random seeds and select the one with max return.

A Proof of Theorem 1

In this section, we present detailed proofs for the theoretical derivation of Thm. 1, which aims to solve the following optimization problem:

$$\begin{aligned} \min_{w_k} \quad & \eta(\pi^*) - \eta(\pi_k) \\ \text{s.t.} \quad & Q_k = \arg \min_{Q \in \mathcal{Q}} \mathbb{E}_\mu[w_k(s, a) \cdot (Q - \mathcal{B}^* Q_{k-1})^2(s, a)], \\ & \mathbb{E}_\mu[w_k(s, a)] = 1, \quad w_k(s, a) \geq 0, \end{aligned} \quad (1)$$

The problem is equivalent to:

$$\begin{aligned} \min_{p_k} \quad & \eta(\pi^*) - \eta(\pi_k) \\ \text{s.t.} \quad & Q_k = \arg \min_{Q \in \mathcal{Q}} \mathbb{E}_{p_k}[(Q - \mathcal{B}^\pi Q_{k-1})^2(s, a)] \\ & \sum_{s, a} p_k(s, a) = 1, \quad p_k(s, a) \geq 0, \end{aligned} \quad (2)$$

The desired $w_k(s, a)$ is $\frac{p_k(s, a)}{\mu(s, a)}$, where $p_k(s, a)$ is the solution to the problem 2.

To solve Problem 2, we need to give the definition of *total variation distance*, *Wasserstein metric* and the diameter of a set, and introduce some mild assumptions.

Definition 1 (total variation distance). *The total variation (TV) distance of distribution P and Q is defined as*

$$D_{\text{TV}}(P, Q) = \frac{1}{2} \|P - Q\|_1$$

Definition 2 (Wasserstein metric). *For F, G two c.dfs over the reals, the Wasserstein metric is defined as*

$$d_p(F, G) := \inf_{U, V} \|U - V\|_p$$

where the infimum is taken over all pairs of random variables (U, V) with respective cumulative distributions F and G.

Definition 3. *The diameter of a set A is defined as*

$$\text{diam}(A) = \sup_{x, y \in A} m(x, y)$$

where m is the metric on A.

Assumption 1. *The state space \mathcal{S} and action space \mathcal{A} are metric spaces with a metric m .*

Assumption 2. *The Q function is continuous with respect to $\mathcal{S} \times \mathcal{A}$.*

Assumption 3. *The transition function T is continuous with respect to $\mathcal{S} \times \mathcal{A}$ in the sense of Wasserstein metric, i.e.,*

$$\lim_{(s, a) \rightarrow (s_0, a_0)} d_p(T(\cdot | s, a), T(\cdot | s_0, a_0)) = 0,$$

where d_p denote the Wasserstein metric.

These assumptions are not strong and can be satisfied in most of environments includes MuJoCo, Atari games and so on.

Let $d_i^\pi(s)$ denote the discounted state distribution, where the state is visited by the agent for the i-th time. that is

$$d_i^\pi(s) = (1 - \gamma) \sum_{t_i=0}^{\infty} \gamma^{t_i} \Pr(s_{t_k} = s, \forall k \in [i]),$$

where $[k] = \{j \in \mathbb{N}_+ : j \leq k\}$. Notably,

$$d^\pi(s) = \sum_{i=1}^{\infty} d_i^\pi(s) \quad (3)$$

$$d_i^\pi(s) = \sum_{t=1}^{\infty} \rho^\pi(s, \pi(s), t) \gamma^t d_{i-1}^\pi(s), \quad (4)$$

where $\rho^\pi(s, \pi(s), t)$ is the shorthand for $\mathbb{E}_{a \sim \pi} \rho^\pi(s, a, t)$.

The standard definitions of Q function, value function and advantage function is:

$$\begin{aligned} Q^\pi(s, a) &= \mathbb{E}_\pi [\sum_{t \geq 0} \gamma^t r(s_t, a_t) | s_0 = s, a_0 = a]. \\ V^\pi(s) &= \mathbb{E}_\pi [\sum_{t \geq 0} \gamma^t r(s_t, a_t) | s_0 = s]. \\ A^\pi(s, a) &= Q^\pi(s, a) - V^\pi(s). \end{aligned}$$

In the follows, Lemma 1 is a technique used in Lemma 2. Lemma 2 shows that $\left| \frac{\partial d^\pi(s)}{\partial \pi(s)} \right|$ is a small quantity.

Lemma 1. Let f be an Lebesgue integrable function, P and Q are two probability distributions, $|f| \leq C$, then

$$|\mathbb{E}_{P(x)} f(x) - \mathbb{E}_{Q(x)} f(x)| \leq CD_{\text{TV}}(P, Q) \quad (5)$$

Proof.

$$\begin{aligned} |\mathbb{E}_{P(x)} f(x) - \mathbb{E}_{Q(x)} f(x)| &= \left| \sum_x [P(x)f(x) - Q(x)f(x)] \right| \\ &= \left| \sum_x [P(x)f(x) - Q(x)f(x)] \mathbb{I}[P(x) > Q(x)] \right. \\ &\quad \left. - \sum_x [P(x)f(x) - Q(x)f(x)] \mathbb{I}[P(x) < Q(x)] \right| \\ &\leq CD_{\text{TV}}(P, Q) \end{aligned}$$

□

Lemma 2. Let $\epsilon_\pi = \sup_{s,a} \sum_{t=1}^{\infty} \gamma^t \rho^\pi(s, a, t)$, we have

$$\left| \frac{\partial d^\pi(s)}{\partial \pi(s)} \right| \leq \epsilon_\pi d_1^\pi(s) \quad (6)$$

and $\epsilon_\pi \leq 1$.

Proof. The definition of $\rho^\pi(s, a, t)$ implies

$$0 \leq \sum_{t=1}^{\infty} \gamma^t \rho^\pi(s, a, t) \leq \epsilon_\pi \leq 1, \quad \forall a \in \mathcal{A}$$

Based on this fact, we have

$$\left| \sum_{t=1}^{\infty} \gamma^t (\rho^\pi(s, a_1, t) - \rho^\pi(s, a_2, t)) \right| \leq \epsilon_\pi, \quad \forall a_1, a_2 \in \mathcal{A}$$

Let $\rho^\pi(s, \pi(s), t)$ be a shorthand for $\mathbb{E}_{a \sim \pi(s)} \rho^\pi(s, a, t)$.

If π changes a little and becomes π' , and $\delta_a = D_{\text{TV}}(\pi(s), \pi'(s))$, then we have

$$\begin{aligned} & \left| \sum_{t=1}^{\infty} \gamma^t (\rho^\pi(s, \pi(s), t) - \rho^\pi(s, \pi'(s), t)) \right| \\ &= \left| \mathbb{E}_{a_1 \sim \pi} \sum_{t=1}^{\infty} \gamma^t \rho^\pi(s, a_1, t) - \mathbb{E}_{a_2 \sim \pi'} \sum_{t=1}^{\infty} \gamma^t \rho^\pi(s, a_1, t) \right| \\ &\leq \epsilon_\pi \delta_a \end{aligned} \tag{7}$$

This inequality comes from Lemma 1.

We denote the difference between $d_2^\pi(s)$ and $d_2^{\pi'}(s)$ as $\Delta d_2(s)$, which can be bounded as follows:

$$\begin{aligned} \Delta d_2(s) &= |d_2^\pi(s) - d_2^{\pi'}(s)| \\ &= \left| \sum_{t=1}^{\infty} \gamma^t (\rho^\pi(s, \pi(s), t) - \rho^\pi(s, \pi'(s), t)) d_1^\pi(s) \right| \\ &= d_1^\pi(s) \left| \sum_{t=1}^{\infty} \gamma^t (\rho^\pi(s, \pi(s), t) - \rho^\pi(s, \pi'(s), t)) \right| \\ &\leq \epsilon_\pi \delta_a d_1^\pi(s) \end{aligned}$$

Recursively, we have

$$\Delta d_i(s) \leq \epsilon_\pi^{i-1} \delta_a^{i-1} d_1^\pi(s)$$

Obviously, the change of π at state s won't change $d_1^\pi(s)$. According to Eq. (3),

$$\begin{aligned} \Delta d(s) &\leq \sum_{i=1}^{\infty} \Delta d_i(s) \\ &\leq \sum_{i=2}^{\infty} (\epsilon_\pi \delta_a)^{i-1} d_1^\pi(s) \\ &= \frac{\epsilon_\pi \delta_a}{1 - \epsilon_\pi \delta_a} d_1^\pi(s) \end{aligned}$$

According to $\frac{\partial d^\pi(s)}{\partial \pi(s)} = \lim_{\delta_a \rightarrow 0} \frac{\Delta d(s)}{\delta_a}$, we have

$$\left| \frac{\partial d^\pi(s)}{\partial \pi(s)} \right| \leq \epsilon_\pi d_1^\pi(s)$$

This concludes the proof. \square

Lemma 3. Given two policy π_1 and π_2 , where $\pi_1(a|s) = \frac{\exp(Q_1(s, a))}{\sum_{a'} \exp(Q_1(s, a'))}$. Then

$$\mathbb{E}_{a \sim \pi_2} Q_1(s, a) - \mathbb{E}_{a \sim \pi_1} Q_1(s, a) \leq 1$$

Proof. Suppose there are two actions a_1, a_2 under state s , and let $Q_1(s, a_1) = u, Q_1(s, a_2) = v$. Without loss of generality, let $u \leq v$.

$$\begin{aligned} \mathbb{E}_{a \sim \pi_2} Q_1(s, a) - \mathbb{E}_{a \sim \pi_1} Q_1(s, a) &\leq v - \frac{ue^u + ve^v}{e^u + e^v} \\ &= v - \frac{u + ve^{v-u}}{1 + e^{v-u}} \\ &= v - u - \frac{(v-u)e^{v-u}}{1 + e^{v-u}} \end{aligned}$$

Let $f(z) = z - \frac{ze^z}{1+e^z}$, the maximum point z_0 of $f(z)$ satisfies $f'(z_0) = 0$ where f' is the derivative of f , i.e., $\frac{e^{z_0}(1+z_0+e^{z_0})}{(1+e^{z_0})^2} - 1 = 0$. This implies $1 + e^{z_0} = z_0 e^{z_0}$ and $z_0 \in (1, 2)$. We have

$$\mathbb{E}_{a \sim \pi_2} Q_1(s, a) - \mathbb{E}_{a \sim \pi_1} Q_1(s, a) \leq f(v - u) \leq z_0 - 1 \leq 1$$

If the number of action is more than 2 and $Q_1(s, a_1) \geq Q_1(s, a_2) \geq \dots \geq Q_1(s, a_n)$, let b_1 represents a_1 and b_2 represents all other actions. Then $Q_1(s, b_1) = Q_1(s, a_1)$ and $Q_1(s, b_2) = \sum_{j=2}^n \frac{Q_1(s, a_j) \exp(Q_1(s, a_j))}{\sum_{k=2}^n \exp(Q_1(s, a_k))}$. In this way, we can derive the upper bound of $\mathbb{E}_{a \sim \pi_2} Q_1(s, a) - \mathbb{E}_{a \sim \pi_1} Q_1(s, a)$ as above. \square

The following lemma is proposed by Kakade,

Lemma 4 (Lemma 6.1 in [?]). *For any policy $\tilde{\pi}$ and π ,*

$$\eta(\tilde{\pi}) - \eta(\pi) = \frac{1}{1-\gamma} \mathbb{E}_{d^{\tilde{\pi}}(s,a)} [A_\pi(s,a)] \quad (8)$$

Lemma 5. *In discrete MDPs, let $\epsilon_{\pi_k} = \sup_{s,a} \sum_{t=1}^{\infty} \gamma^t \rho^{\pi_k}(s, a, t)$, the optimal solution p_k to a relaxation of optimization problem 2 satisfies the following relationship:*

$$p_k(s, a) = \frac{1}{Z^*} (D_k(s, a) + \epsilon_k(s, a)) \quad (9)$$

where $D_k(s, a) = d^{\pi_k}(s, a)(2 - \pi_k(a|s)) \exp(-|Q_k - Q^*(s, a)|) |Q_k - \mathcal{B}^* Q_{k-1}|(s, a)$, Z^* is the normalization constant and $\frac{\epsilon_k(s, a)}{D_k(s, a)} \leq \epsilon_{\pi_k}$.

Proof. Suppose $a^* \sim \pi^*(s)$. Let $\pi = \pi_k$, $\tilde{\pi} = \pi^*$ in Lemma 4, we have

$$\begin{aligned} & \eta(\pi^*) - \eta(\pi_k) \\ &= -\frac{1}{1-\gamma} \mathbb{E}_{d^{\pi_k}(s,a)} A_{\pi^*}(s,a) \\ &= \frac{1}{1-\gamma} \mathbb{E}_{d^{\pi_k}(s,a)} (V^*(s) - Q^*(s, a)) \\ &= \frac{1}{1-\gamma} \mathbb{E}_{d^{\pi_k}(s,a)} (V^*(s) - Q_k(s, a^*) + Q_k(s, a^*) - Q_k(s, a) + Q_k(s, a) - Q^*(s, a)) \quad (10) \\ &\stackrel{(a)}{\leq} \frac{1}{1-\gamma} \left(\mathbb{E}_{d^{\pi_k}(s)} (Q^*(s, a^*) - Q_k(s, a^*)) + \mathbb{E}_{d^{\pi_k}(s,a)} (Q_k(s, a) - Q^*(s, a)) + 1 \right) \\ &\leq \frac{1}{1-\gamma} \left(\mathbb{E}_{d^{\pi_k}(s)} |Q^*(s, a^*) - Q_k(s, a^*)| + \mathbb{E}_{d^{\pi_k}(s,a)} |Q_k(s, a) - Q^*(s, a)| + 1 \right) \\ &= \frac{2}{1-\gamma} \left(\mathbb{E}_{d^{\pi_k}, \pi^*} |Q_k(s, a) - Q^*(s, a)| + 1 \right), \end{aligned}$$

where $d^{\pi_k, \pi^*}(s, a) = d^{\pi_k}(s) \frac{\pi_k(a|s) + \pi^*(a|s)}{2}$ and (a) uses Lemma 3.

Since both sides of the above equation have the same minimum (here the minima are given by $Q_k = Q^*$), we can replace the objective in Problem 2 with the upper bound in Eq. (10) and solve the relaxed optimization problem.

$$\min_{p_k} \quad \mathbb{E}_{d^{\pi_k}(s,a)} [|Q_k - Q^*|] \quad (11)$$

$$\text{s.t.} \quad Q_k = \arg \min_{Q \in \mathcal{Q}} \mathbb{E}_{p_k} [(Q - \mathcal{B}^\pi Q_{k-1})^2(s, a)], \quad (12)$$

$$\sum_{s,a} p_k(s, a) = 1, \quad p_k(s, a) \geq 0. \quad (13)$$

Here we use $d^{\pi_k}(s, a)$ to replace d^{π_k, π^*} because we can not access π^* , and the best surrogate available is π_k .

Step 1: Jensen's Inequality. The optimization objective can be further relaxed with Jensen's Inequality, based on the fact that $f(x) = \exp(-x)$ is a convex function.

$$\mathbb{E}_{d^{\pi_k}(s,a)} [|Q_k - Q^*|] = -\log \exp(-\mathbb{E}_{d^{\pi_k}(s,a)} [|Q_k - Q^*|]) \leq -\log \mathbb{E}_{d^{\pi_k}(s,a)} [\exp(-|Q_k - Q^*|)] \quad (14)$$

Similarly, both sides of Eq. (14) have the same minimum. We obtain the following new optimization problem by replacing the objective with the upper bound in this equation:

$$\begin{aligned} \min_{p_k} & -\log \mathbb{E}_{d^{\pi_k}(s,a)}[\exp(-|Q_k - Q^*|)] \\ \text{s.t. } & Q_k = \arg \min_{Q \in \mathcal{Q}} \mathbb{E}_{p_k}[(Q - \mathcal{B}^* Q_{k-1})^2], \\ & \sum_{s,a} p_k(s,a) = 1, \quad p_k(s,a) \geq 0. \end{aligned} \tag{15}$$

Step 2: Computing the Lagrangian. In order to optimize problem 15, we follow the standard procedures of Lagrangian multiplier method. The Lagrangian is:

$$\mathcal{L}(p_k; \lambda, \mu) = -\log \mathbb{E}_{d^{\pi_k}(s,a)}[\exp(-|Q_k - Q^*|)] + \lambda(\sum_{s,a} p_k(s,a) - 1) - \mu^T p_k. \tag{16}$$

where λ and μ are the Lagrange multipliers.

Step 3: IFT gradient used in the Lagrangian. $\frac{\partial Q_k}{\partial p_k}$ can be computed according to implicit function theorem (IFT). The IFT gradient is given by:

$$\left. \frac{\partial Q_k}{\partial p_k} \right|_{Q_k, p_k} = -[\text{Diag}(p_k)]^{-1} [\text{Diag}(Q_k - \mathcal{B}^* Q_{k-1})] \tag{17}$$

The derivation is similar to that in [?].

Step 4: Approximation of the gradient used in the Lagrangian. We derive an expression for $\frac{\partial d^{\pi_k}(s,a)}{\partial p_k}$, which will be used when computing the gradient of the Lagrangian. We use π_k to denote the policy induced by Q_k .

$$\begin{aligned} \frac{\partial d^{\pi_k}(s,a)}{\partial p_k} &= \frac{\partial d^{\pi_k}(s,a)}{\partial \pi_k} \frac{\partial \pi_k}{\partial Q_k} \frac{\partial Q_k}{\partial p_k} \\ &= (d^{\pi_k}(s) + \epsilon_2(s)) \frac{\partial \pi_k}{\partial Q_k} \frac{\partial Q_k}{\partial p_k} \\ &\stackrel{(b)}{=} (d^{\pi_k}(s) + \epsilon_2(s)\pi_k(a|s)) \frac{\sum_{a' \neq a} \exp(Q_k(s,a'))}{\sum_{a'} \exp(Q_k(s,a'))} \frac{\partial Q_k}{\partial p_k} \\ &\stackrel{(c)}{=} d^{\pi_k}(s,a)(1 - \pi_k(a|s)) \frac{\partial Q_k}{\partial p_k} + \epsilon_2(s)\pi_k(a|s)(1 - \pi_k(a|s)) \frac{\partial Q_k}{\partial p_k} \end{aligned}$$

where $\epsilon_2(s) = \frac{\partial d^{\pi_k}(s)}{\partial \pi_k(s)}$. (b) and (c) are based on the fact that $\pi_k(a|s) = \frac{\exp(Q_k(s,a))}{\sum_{a'} \exp(Q_k(s,a'))}$.

Step 5: Computing optimal p_k . By KKT conditions, we have

$$\frac{\partial \mathcal{L}(p_k; \lambda, \mu)}{\partial p_k} = 0$$

$$\begin{aligned} & \frac{\partial \mathcal{L}(p_k; \lambda, \mu)}{\partial p_k} \\ &= \frac{\exp(-|Q_k - Q^*|(s,a))}{Z} (d^{\pi_k}(s,a) \text{sgn}(Q_k - Q^*) \cdot \frac{\partial Q_k}{\partial p_k} + \cdot \frac{\partial d^{\pi_k}(s,a)}{\partial p_k}) + \lambda - \mu_{s,a} \end{aligned}$$

where $Z = \mathbb{E}_{s',a' \sim d^{\pi_k}(s,a)} \exp(-|Q_k - Q^*|(s',a'))$. Substituting the expression of $\frac{\partial Q_k}{\partial p_k}$ and $\frac{\partial d^{\pi_k}(s,a)}{\partial p_k}$ with the results obtained in Step. 3 and Step. 4 respectively, and let $Z_{s,a} = Z(\lambda^* - \mu_{s,a}^*)$, we obtain

$$\begin{aligned} p_k(s,a) &= \left(d^{\pi_k}(s,a) (\text{sgn}(Q_k - Q^*) + 1 - \pi_k(a|s)) \exp(-|Q_k - Q^*|(s,a)) |Q_k - \mathcal{B}^* Q_{k-1}|(s,a) \right. \\ &\quad \left. + \epsilon_2(s)\pi_k(a|s)(1 - \pi_k(a|s)) \exp(-|Q_k - Q^*|(s,a)) |Q_k - \mathcal{B}^* Q_{k-1}|(s,a) \right) \frac{1}{Z_{s,a}} \end{aligned} \tag{18}$$

Notably, $Q_k \approx Q^{\pi_k} \leq Q^*$. Thus, $\text{sgn}(Q_k - Q^*)$ always is 1 approximately, so we can simplify this relationship as

$$p_k(s, a) = \frac{1}{Z_{s,a}} \left(d^{\pi_k}(s, a)(2 - \pi_k(a|s)) \exp(-|Q_k - Q^*|(s, a)) |Q_k - \mathcal{B}^* Q_{k-1}|(s, a) \right. \\ \left. + \epsilon_2(s)\pi_k(a|s)(1 - \pi_k(a|s)) \exp(-|Q_k - Q^*|(s, a)) |Q_k - \mathcal{B}^* Q_{k-1}|(s, a) \right) \quad (19)$$

The first term is always larger or equal to zero. The second term does not influence the sign of the equation because the absolute value of $\epsilon_2(s)$ is smaller than $d^{\pi_k}(s)$ according to Lemma 2. Note that Eq. (19) is always larger or equal to zero. If it is larger than zero then $\mu^* = 0$ by the KKT condition. If it is equal to zero, we can let $\mu^* = 0$ because the value of μ^* does not influence $w_k(s, a)$. Without loss of generality, we can let $\mu^* = 0$. Then $Z_{s,a} = Z^* = Z\lambda^*$ is a constant with respect to different s and a . In this way, we can simplify Eq. (19) as follows:

$$p_k(s, a) = \frac{1}{Z^*} (D_k(s, a) + \epsilon_k(s, a))$$

where $D_k(s, a) = d^{\pi_k}(s, a)(2 - \pi_k(a|s)) \exp(-|Q_k - Q^*|(s, a)) |Q_k - \mathcal{B}^* Q_{k-1}|(s, a)$ and $\epsilon_k(s, a) = \epsilon_2(s)\pi_k(a|s)(1 - \pi_k(a|s)) \exp(-|Q_k - Q^*|(s, a)) |Q_k - \mathcal{B}^* Q_{k-1}|(s, a)$.

Based on the expression of $D_k(s, a)$ and $\epsilon_k(s, a)$, we have

$$\frac{\epsilon_k(s, a)}{D_k(s, a)} = \frac{\epsilon_2(s)(1 - \pi_k(a|s))}{d^{\pi_k}(s)(2 - \pi_k(a|s))} \leq \epsilon_{\pi_k}$$

The inequality is from 2. This concludes the proof. \square

Theorem 1 (formal). Let $\epsilon_{\pi_k} = \sup_{s,a} \sum_{t=1}^{\infty} \gamma^t \rho^{\pi_k}(s, a, t)$. Under Assumption 1, 2 and 3, if $\frac{d^{\pi_k}(s,a)}{\mu(s,a)}$ exists, we have in MDPs with discrete action spaces, the solution w_k to the relaxed optimization problem 1 is

$$w_k(s, a) = \frac{1}{Z_1^*} (E_k(s, a) + \epsilon_{k,1}(s, a)). \quad (20)$$

In MDPs with continuous action spaces, the solution is

$$w_k(s, a) = \frac{1}{Z_2^*} (F_k(s, a) + \epsilon_{k,2}(s, a)). \quad (21)$$

where

$$E_k(s, a) = \frac{d^{\pi_k}(s, a)}{\mu(s, a)} (2 - \pi_k(a|s)) \exp(-|Q_k - Q^*|(s, a)) |Q_k - \mathcal{B}^* Q_{k-1}|(s, a)$$

$$F_k(s, a) = 2 \frac{d^{\pi_k}(s, a)}{\mu(s, a)} \exp(-|Q_k - Q^*|(s, a)) |Q_k - \mathcal{B}^* Q_{k-1}|(s, a),$$

Z_1^*, Z_2^* is the normalization constants and $\max \left\{ \frac{\epsilon_{k,1}(s,a)}{E_k(s,a)}, \frac{\epsilon_{k,2}(s,a)}{F_k(s,a)} \right\} \leq \epsilon_{\pi_k}$.

Proof. By Lemma 5, for MDPs with discrete action space and state space, we have

$$p_k(s, a) = \frac{1}{Z^*} (D_k(s, a) + \epsilon_k(s, a))$$

Based on the deviation of Problem 2, the solution in this situation is

$$w_k(s, a) = \frac{1}{Z^*} \left(\frac{D_k(s, a)}{\mu(s, a)} + \frac{\epsilon_k(s, a)}{\mu(s, a)} \right) \quad (22)$$

The existence of $\frac{d^{\pi_k}(s,a)}{\mu(s,a)}$ guarantees the existence of $\frac{D_k(s,a)}{\mu(s,a)}$ and $\frac{\epsilon_k(s,a)}{\mu(s,a)}$. Let $E_k(s, a) = \frac{D_k(s,a)}{\mu(s,a)}$ and $\epsilon_{k,1}(s, a) = \frac{\epsilon_k(s,a)}{\mu(s,a)}$, we get Eq. (20).

We derive the result for continuous action space and state space as follows, the result for continuous state space and discrete action space, and discrete state space and continuous action space can be derived similarly.

Remember that $\mathcal{B}^*Q_{k-1}(s, a) = r(s, a) + \gamma \max_{a'} \mathbb{E}_{s'} Q_{k-1}(s', a')$ and $Q_k(s, a) = \arg \min_Q (Q(s, a) - \mathcal{B}^*Q_{k-1}(s, a))^2$, if we use $R(s, a) = Q_k(s, a) - \gamma \max_{a'} \mathbb{E}_{s'} Q_{k-1}(s', a')$ to replace $r(s, a)$, then Q_k is still the desired Q function after the Bellman update. Since the continuity of Q_k , Q_{k-1} and T guarantee $R(s, a)$ is continuous, without loss of generality, we assume $r(s, a)$ is continuous.

We utilize the techniques in reinforcement learning with aggregated states [?]. Concretely, we can partition the set of all state-action pairs, with each cell representing an aggregated state. Such a partition can be defined by a function $\phi : \mathcal{S} \cup \mathcal{A} \mapsto \hat{\mathcal{S}} \cup \hat{\mathcal{A}}$, where $\hat{\mathcal{S}}$ is the space of aggregated states and $\hat{\mathcal{A}}$ is the space of aggregated actions. With such a partition, we can discretize the continuous spaces. For example, for the continuous space $\{x \in \mathbb{R} : 0 \leq x \leq 10\}$, define $\phi(x) = \sum_{i=1}^9 \mathbb{I}(x \leq x_i)$, and then the space of aggregated states becomes $\{0, 1, 2, \dots, 9\}$, which is a discrete space.

With function ϕ , we define the transition function and reward function in this new MDP. For all $\hat{s}, \hat{s}' \in \hat{\mathcal{S}}, \hat{a} \in \hat{\mathcal{A}}$

$$\begin{aligned}\hat{T}(\hat{s}'|\hat{s}, \hat{a}) &= \frac{\sum_{s,a \in \phi^{-1}(\hat{s}, \hat{a})} \mu(s, a) \sum_{s' \in \phi^{-1}(\hat{s}')} T(s'|s, a)}{\sum_{s,a \in \phi^{-1}(\hat{s}, \hat{a})} \mu(s, a)} \\ \hat{r}(\hat{s}, \hat{a}) &= \frac{\sum_{s,a \in \phi^{-1}(\hat{s}, \hat{a})} \mu(s, a) r(s, a)}{\sum_{s,a \in \phi^{-1}(\hat{s}, \hat{a})} \mu(s, a)}\end{aligned}\tag{23}$$

where $(\phi(s), \phi(a))$ is simplified as $\phi(s, a)$ and $\phi^{-1}(\hat{s}, \hat{a})$ is the preimage of (\hat{s}, \hat{a}) .

In this way, Eq. (22) holds for aggregated state space:

$$\hat{w}_k(\phi(s, a)) = \frac{1}{\hat{Z}^*} \left(\frac{\hat{D}_k(\phi(s, a))}{\hat{\mu}(\phi(s, a))} + \frac{\hat{\epsilon}_k(\phi(s, a))}{\hat{\mu}(\phi(s, a))} \right)\tag{24}$$

Suppose $\hat{\mathcal{S}}$ and $\hat{\mathcal{A}}$ is equipped with metric m' , we construct a sequence of functions ϕ_h , which satisfies

- (i) If $m(u_1 - u_2) \leq m(u_1 - u_3)$, then $m'(\phi_h(u_1) - \phi_h(u_2)) \leq m'(\phi_h(u_1) - \phi_h(u_3))$ for all $u_1, u_2, u_3 \in \mathcal{S}$ or $u_1, u_2, u_3 \in \mathcal{A}$.
- (ii) $\lim_{h \rightarrow \infty} \text{diam}(\phi_h^{-1}(c)) = 0$ for all $c \in \mathcal{S}' \cup \mathcal{A}'$.

Based on the two conditions on ϕ_h and the continuous of reward function and transition function, for all $s, s' \in \mathcal{S}$ and $a \in \mathcal{A}$,

$$\begin{aligned}\lim_{h \rightarrow \infty} |\hat{r}(\phi_h(s, a)) - r(s, a)| &= 0 \\ \lim_{h \rightarrow \infty} |\hat{T}(\phi_h(s')|\phi_h(s, a)) - T(s'|s, a)| &= 0\end{aligned}\tag{25}$$

This means the constructed MDP approaches the original MDP as h tends to infinity.

With the Lemma 3 in [?],

$$\begin{aligned}\lim_{h \rightarrow \infty} \mathcal{B}^*\hat{Q}_{k-1}(\phi_h(s, a)) &= \mathcal{B}^*Q_{k-1}(s, a) \\ \lim_{h \rightarrow \infty} \mathcal{B}^*\hat{Q}^*(\phi_h(s, a)) &= \mathcal{B}^*Q^*(s, a)\end{aligned}$$

Note that $Q_k(s, a) = \arg \min_Q (Q - \mathcal{B}^*Q_{k-1}(s, a))^2$, $\hat{Q}_k(\phi_h(s, a)) = \arg \min_Q (Q - \mathcal{B}^*\hat{Q}_{k-1}(\phi_h(s, a)))^2$, $Q^*(s, a) = \arg \min_Q (Q - \mathcal{B}^*Q^*(s, a))^2$ and $\hat{Q}^*(\phi_h(s, a)) = \arg \min_Q (Q - \mathcal{B}^*\hat{Q}^*(\phi_h(s, a)))^2$,

$$\begin{aligned}\lim_{h \rightarrow \infty} \hat{Q}_k(\phi_h(s, a)) &= Q_k(s, a) \\ \lim_{h \rightarrow \infty} \hat{Q}^*(\phi_h(s, a)) &= Q^*(s, a)\end{aligned}$$

Because $\pi(a|s) = \frac{\exp(Q(s,a))}{\sum_{a'} \exp(Q(s,a'))}$, π is continuous with respect to Q , then we have

$$\lim_{h \rightarrow \infty} \hat{\pi}_k(\phi_h(a)|\phi_h(s)) = \pi_k(a|s)$$

The continuity of π and transition function T guarantees

$$\lim_{h \rightarrow \infty} \hat{d}^{\hat{\pi}_k}(\phi_h(s, a)) = d^{\pi_k}(s, a)$$

Therefore,

$$\begin{aligned} \lim_{h \rightarrow \infty} |\hat{Q}_k - \hat{Q}^*|(\phi((s, a))) &= |Q_k - Q^*|(s, a) \\ \lim_{h \rightarrow \infty} |\hat{Q}_k - \hat{\mathcal{B}}^* \hat{Q}^*|(\phi((s, a))) &= |Q_k - \mathcal{B}^* Q_{k-1}|(s, a) \\ \lim_{h \rightarrow \infty} \frac{d^{\hat{\pi}_k}(\phi_h(s, a))}{\hat{\mu}(\phi_h(s, a))} &= \frac{d^{\pi_k}(s, a)}{\mu(s, a)} \end{aligned} \quad (26)$$

Notably, $\epsilon_2(s)\pi_k(a|s) \leq d^{\pi_k}(s, a)$, the existence of $\frac{d^{\pi_k}(s, a)}{\mu(s, a)}$ implies the existence of $\frac{\epsilon_2(s)\pi_k(a|s)}{\mu(s, a)}$.

$$\lim_{h \rightarrow \infty} \frac{\hat{\epsilon}_k(\phi(s, a))}{\hat{\mu}(\phi(s, a))} = \epsilon_{k,1}(s, a) \quad (27)$$

where $\epsilon_{k,1} = \frac{\epsilon_k(s)\pi_k(a|s)}{\mu(s, a)}(1 - \pi_k(a|s)) \exp(-|Q_k - Q^*|(s, a)) |Q_k - \mathcal{B}^* Q_{k-1}|(s, a)$.

Using the Eq. (A), (26) and (27), we have

$$w_k(s, a) = \frac{1}{Z_1^*} (E_k(s, a) + \epsilon_{k,1}(s, a)).$$

If the action space is continuous, $\pi_k(a|s) = 0$, then we have

$$w_k(s, a) = \frac{1}{Z_2^*} (F_k(s, a) + \epsilon_{k,2}(s, a))$$

The upper bound of $\frac{\epsilon_{k,1}(s, a)}{E_k(s, a)}$ and $\frac{\epsilon_{k,2}(s, a)}{F_k(s, a)}$ can be derived directly from Lemma 5. This concludes our proof. \square

B Detailed Proof of Theorem ??

Let $(\mathcal{B}Q)_k(s, a)$ denote $|Q_k(s, a) - \mathcal{B}^* Q_k(s, a)|$. We first introduce an assumption.

Assumption 4. At iteration k , $(\mathcal{B}Q)_k(s, a)$ is independent of $(\mathcal{B}Q)_k(s', a')$ if $(s, a) \neq (s', a')$ for all $k > 0$.

This assumption is not strong. If we use a table to represent Q function, it holds apparently. Notably, though we need this assumption in our proof, we can also apply our method on the situation where this assumption doesn't hold. With this assumption, we have the following theorem.

Lemma 6. Consider a MDP, trajectories $\tau_i = \{s_t^i, a_t^i\}_{t=0}^{T_i}, i = 0, 1, \dots$ is generated by a policy π under this MDP, then we have

$$\begin{aligned} |Q_k(s, a) - Q^*(s, a)| &\leq |Q_k(s_t, a_t) - \mathcal{B}^* Q_{k-1}(s_t, a_t)| \\ &\quad + \mathbb{E}_\tau \left(\sum_{t'=1}^{h_\tau^{\pi_k}(s, a)} \gamma^{t'} \left((\mathcal{B}Q)_{k-1}(s_{t'}, a_{t'}) + c \right) + \gamma^{h_\tau^{\pi_k}(s, a)+1} c \right) \end{aligned} \quad (28)$$

where $(\mathcal{B}Q)_k(s_{h_\tau^{\pi_k}(s, a)}, a_{h_\tau^{\pi_k}(s, a)}) = |Q_k(s_{h_\tau^{\pi_k}(s, a)}, a_{h_\tau^{\pi_k}(s, a)}) - r(s_{h_\tau^{\pi_k}(s, a)}, a_{h_\tau^{\pi_k}(s, a)})|$, $c = \max_{s,a} (Q^*(s, a^*) - Q^*(s, a))$, and $(s_{t'}, a_{t'})$ is the t' -th state-action pair behind (s, a) .

Proof.

$$\begin{aligned}
& |Q_k(s_t, a_t) - Q^*(s_t, a_t)| \\
&= |Q_k(s_t, a_t) - \mathcal{B}^*Q_{k-1}(s_t, a_t) + \mathcal{B}^*Q_{k-1}(s_t, a_t) - \mathcal{B}^*Q^*(s_t, a_t)| \\
&\stackrel{(a)}{\leq} |Q_k(s_t, a_t) - \mathcal{B}^*Q_{k-1}(s_t, a_t)| \\
&\quad + \gamma |\mathbb{E}_{p(\tau)}[Q_{k-1}(s_{t+1}, a_{t+1}) - Q^*(s_{t+1}, a_{t+1}) + Q^*(s_{t+1}, a_{t+1}) - Q^*(s_{t+1}, a^*)]| \\
&\stackrel{(b)}{\leq} |Q_k(s_t, a_t) - \mathcal{B}^*Q_{k-1}(s_t, a_t)| + \gamma c + \gamma \mathbb{E}_\tau [|Q_{k-1}(s_{t+1}, a_{t+1}) - Q^*(s_{t+1}, a_{t+1})|]
\end{aligned}$$

where the expectation is taken over $s' \sim P(s'|s, a)$, $a' \sim \pi(a'|s')$. (a) uses triangle inequality, (b) is because $f(x) = |x|$ is convex function and using Jensen's Inequality.

Similarly, we have

$$\begin{aligned}
& |Q_{k-1}(s_{t+1}, a_{t+1}) - Q^*(s_{t+1}, a_{t+1})| \\
&= |Q_{k-1}(s_{t+1}, a_{t+1}) - \mathcal{B}^*Q_{k-1}(s_{t+1}, a_{t+1}) + \mathcal{B}^*Q_{k-1}(s_{t+1}, a_{t+1}) - \mathcal{B}^*Q^*(s_{t+1}, a_{t+1})| \\
&\leq (\mathcal{B}Q)_{k-1}(s_{t+1}, a_{t+1}) + \gamma c + \gamma \mathbb{E}_\tau [|Q_{k-1}(s_{t+2}, a_{t+2}) - Q^*(s_{t+2}, a_{t+2})|]
\end{aligned}$$

Recursively,

$$\begin{aligned}
& |Q_k(s, a) - Q^*(s, a)| \\
&\leq |Q_k(s_t, a_t) - \mathcal{B}^*Q_{k-1}(s_t, a_t)| + \sum_{t'=1}^{h_\tau^{\pi_k}(s, a)} \gamma^{t'} \left((\mathcal{B}Q)_{k-1}(s_{t'}, a_{t'}) + c \right) + \gamma^{h_\tau^{\pi_k}(s, a)+1} c \quad (29)
\end{aligned}$$

where $(\mathcal{B}Q)_{k-1}(s_{h_\tau^{\pi_k}(s, a)}, a_{h_\tau^{\pi_k}(s, a)}) = |Q_{k-1}(s_{h_\tau^{\pi_k}(s, a)}, a_{h_\tau^{\pi_k}(s, a)}) - r(s_{h_\tau^{\pi_k}(s, a)}, a_{h_\tau^{\pi_k}(s, a)})|$. \square

This theorem shows that the cumulative Bellman error with a constant c is an upper bound of $|Q_k - Q^*|$, so we can use Bellman error with the constant to estimate this quantity.

Suppose the Q function is equipped with a learning rate α , i.e., $Q_k = \alpha(\mathcal{B}^*Q_{k-1} - Q_{k-1}) + (1 - \alpha)Q_{k-1}$, we have the following lemma,

Lemma 7.

$$\begin{aligned}
\|\mathcal{B}^*Q_k - Q_k\|_\infty &\leq (\alpha\gamma + 1 - \alpha)^k \|\mathcal{B}^*Q_0 - Q_0\|_\infty \\
\|\mathcal{B}^*Q_{k-1} - Q_k\|_\infty &\leq (1 - \alpha)(\alpha\gamma + 1 - \alpha)^{k-1} \|\mathcal{B}^*Q_0 - Q_0\|_\infty \quad (30)
\end{aligned}$$

Proof.

$$\begin{aligned}
Q_k &= Q_{k-1} + \alpha(\mathcal{B}^*Q_{k-1} - Q_{k-1}) \\
\implies \mathcal{B}^*Q_{k-1} - Q_k &= \frac{1 - \alpha}{\alpha}(Q_k - Q_{k-1})
\end{aligned}$$

$$\begin{aligned}
\|\mathcal{B}^*Q_k - Q_k\|_\infty &\leq \|\mathcal{B}^*Q_k - \mathcal{B}^*Q_{k-1}\|_\infty + \|\mathcal{B}^*Q_{k-1} - Q_k\|_\infty \\
&\leq \gamma \|Q_k - Q_{k-1}\|_\infty + \|\mathcal{B}^*Q_{k-1} - Q_k\|_\infty \\
&\leq \left(\gamma + \frac{1 - \alpha}{\alpha} \right) \|Q_k - Q_{k-1}\|_\infty \\
&\leq (\alpha\gamma + 1 - \alpha) \|\mathcal{B}^*Q_{k-1} - Q_{k-1}\|_\infty \quad (31)
\end{aligned}$$

$$\begin{aligned}
\|Q_k - \mathcal{B}^*Q_{k-1}\|_\infty &\leq (1 - \alpha) \|Q_{k-1} - \mathcal{B}^*Q_{k-1}\|_\infty \\
&\leq (1 - \alpha) (\|Q_{k-1} - \mathcal{B}^*Q_{k-2}\|_\infty + \|\mathcal{B}^*Q_{k-2} - \mathcal{B}^*Q_{k-1}\|_\infty) \\
&\leq (1 - \alpha) (\gamma \|Q_{k-2} - Q_{k-1}\|_\infty + \|Q_{k-1} - \mathcal{B}^*Q_{k-2}\|_\infty) \\
&\stackrel{(a)}{\leq} (1 - \alpha) \left(\gamma + \frac{1 - \alpha}{\alpha} \right) \|Q_{k-1} - Q_{k-2}\|_\infty \\
&\leq (1 - \alpha)(\alpha\gamma + 1 - \alpha) \|\mathcal{B}^*Q_{k-2} - Q_{k-2}\|_\infty \quad (32)
\end{aligned}$$

Then we can finish the proof by recursively applying Eq. (31) and (32). \square

Lemma 8 (Azuma). *Let X_0, X_1, \dots be a martingale such that, for all $k \geq 1$, $|X_k - X_{k-1}| \leq c_k$. Then*

$$\Pr[|X_n - X_0| \geq t] \leq 2 \exp\left(-\frac{t^2}{2 \sum_{k=1}^n c_k^2}\right). \quad (33)$$

In the follows, we denote $\sum_{t=1}^{h_\tau^{\pi_k}(s,a)} \gamma^t (\mathcal{B}Q)_k(s_t, a_t)$ as $\mathcal{B}(s, a, k)$.

Lemma 9. *Let $\phi_k = (\alpha\gamma + 1 - \alpha)^k \|\mathcal{B}^* Q_0 - Q_0\|_\infty$, $f(t) = \frac{\gamma - \gamma^{t+1}}{1-\gamma}$ and $\epsilon_{\pi_k} = \sup_{s,a} \sum_{t=1}^{\infty} \gamma^t \rho^{\pi_k}(s, a, t)$. Under Assumption 4, with probability at least $1 - \delta$,*

$$|\mathcal{B}(s, a, k) - f(h_\tau^{\pi_k}(s, a)) \mathbb{E}[(\mathcal{B}Q)_k(s_t, a_t)]| \leq \sqrt{2f(h_\tau^{\pi_k}(s, a))^2 (1 + \epsilon_{\pi_k})^2 \phi_k^2 \log \frac{2}{\delta}}. \quad (34)$$

Proof. Let $\mathcal{F}_h = \sigma_t(s_0, a_0, r_0, \dots, s_{h-1}, a_{h-1}, r_{h-1})$ be the σ -field summarising the information available just before s_t is observed.

Define $Y_h = \mathbb{E}[\mathcal{B}(s, a, k) | \mathcal{F}_h]$, then Y_h is a martingale because

$$\mathbb{E}[Y_h | \mathcal{F}_{h-1}] = \mathbb{E}[\mathbb{E}[\mathcal{B}(s, a, k) | \mathcal{F}_h] | \mathcal{F}_{h-1}] = \mathbb{E}[\mathcal{B}(s, a, k) | \mathcal{F}_{h-1}] = Y_{h-1}$$

$$\begin{aligned} |Y_h - Y_{h-1}| &\leq \gamma^h (1 + \epsilon_{\pi_k}) \|\mathcal{B}^* Q_k - Q_k\|_\infty \\ &\leq \gamma^h (1 + \epsilon_{\pi_k}) (\alpha\gamma + 1 - \alpha)^k \|\mathcal{B}^* Q_0 - Q_0\|_\infty = \gamma^h (1 + \epsilon_{\pi_k}) \phi_k \end{aligned}$$

By Azuma's lemma,

$$\Pr\left(|\mathcal{B}(s, a, k) - \mathbb{E}[\mathcal{B}(s, a, k)]| \geq \sqrt{2 \left(\frac{\gamma - \gamma^{h_\tau^{\pi_k}+1}}{1-\gamma}\right)^2 (1 + \epsilon_{\pi_k})^2 \phi_k^2 \log \frac{2}{\delta}}\right) \leq \delta$$

□

Since $(\alpha\gamma + 1 - \alpha)$ is less than 1, ϕ_k decreases exponentially as k increases. This theorem shows that we can use the average Bellman error as a surrogate of Bellman error at specific state-action pair without losing too much accuracy. In this way, $|Q_k - Q^*(s, a)|$ is merely related to the distance to end of the state-action pair.

Theorem 2 (formal). *Under Assumption 4, with probability at least $1 - \delta$, we have*

$$\begin{aligned} &|Q_k(s, a) - Q^*(s, a)| \\ &\leq \mathbb{E}_\tau \left(f(h_\tau^{\pi_k}(s, a)) (\mathbb{E}[(\mathcal{B}Q)_k(s_{t'}, a_{t'})] + c) + \gamma^{h_\tau^{\pi_k}(s,a)+1} c \right) + g(k, \delta) \end{aligned} \quad (35)$$

where $g(k, \delta) = (1 - \alpha)\phi_{k-1} + \sqrt{2f(h_\tau^{\pi_k}(s, a))^2 (1 + \epsilon_{\pi_k})^2 \phi_k^2 \log \frac{2}{\delta}}$.

Proof. According to Lemma 6, we have

$$\begin{aligned} |Q_k(s, a) - Q^*(s, a)| &\leq |Q_k(s_t, a_t) - \mathcal{B}^* Q_{k-1}(s_t, a_t)| \\ &\quad + \mathbb{E}_\tau \left(\sum_{t'=1}^{h_\tau^{\pi_k}(s,a)} \gamma^{t'} \left((\mathcal{B}Q)_{k-1}(s_{t'}, a_{t'}) + c \right) + \gamma^{h_\tau^{\pi_k}(s,a)+1} c \right) \end{aligned} \quad (36)$$

Using Lemma 7, we can upper bound $|Q_k(s_t, a_t) - \mathcal{B}^* Q_{k-1}(s_t, a_t)|$ as $(1 - \alpha)\phi_{k-1}$. With Lemma 9, $\sum_{t=1}^{h_\tau^{\pi_k}(s,a)} \gamma^t (\mathcal{B}Q)_k(s_t, a_t)$ can be bounded by right hand side of Eq. (34) with probability $1 - \delta$.

Substitute the bounds into Eq. (36), we have

$$\begin{aligned}
|Q_k(s, a) - Q^*(s, a)| &\leq (1 - \alpha)\phi_{k-1} + \sqrt{2f(h_\tau^{\pi_k}(s, a))^2(1 + \epsilon_{\pi_k})^2\phi_k^2 \log \frac{2}{\delta}} \\
&\quad + \mathbb{E}_\tau \left(f(h_\tau^{\pi_k}(s, a))(\mathbb{E}[(\mathcal{B}Q)_k(s_{t'}, a_{t'})] + c) + \gamma^{h_\tau^{\pi_k}(s, a)+1}c \right) \\
&\leq g(k, \delta) \\
&\quad + \mathbb{E}_\tau \left(f(h_\tau^{\pi_k}(s, a))(\mathbb{E}[(\mathcal{B}Q)_k(s_{t'}, a_{t'})] + c) + \gamma^{h_\tau^{\pi_k}(s, a)+1}c \right)
\end{aligned}$$

□

C Algorithms

Algorithm 1 ReMERN

- 1: Initialize Q-values $Q_\theta(s, a)$, a replay buffer μ , an **error model** $\Delta_\phi(s, a)$, and a **weight model** κ_ψ .
- 2: **for** step k in $\{1, \dots, N\}$ **do**
- 3: Collect M samples using π_k , add them to replay buffer μ , sample $\{(s_i, a_i)\}_{i=1}^N \sim \mu$.
- 4: Evaluate $Q_\theta(s, a)$, $\Delta_\phi(s, a)$ and $\kappa_\psi(s, a)$ on samples (s_i, a_i) .
- 5: Compute target values for Q and Δ on samples:
 $y_i = r_i + \gamma \max_{a'} Q_{k-1}(s'_i, a')$.
 $\hat{a}_i = \arg \max_a Q_{k-1}(s'_i, a)$.
 $\hat{\Delta} = |Q_\theta(s, a) - y_i| + \gamma \Delta_{k-1}(s'_i, \hat{a}_i)$.
- 6: **Optimize** κ_ψ using

$$L_\kappa(\psi) := \mathbb{E}_{\mathcal{D}_s} [f^*(f'(\kappa_\psi(s, a)))] - \mathbb{E}_{\mathcal{D}_f} [f'(\kappa_\psi(s, a))].$$

- 7: **Compute** w_k using

$$w_k(s, a) \propto \frac{d^{\pi_k}(s, a)}{\mu(s, a)} \exp \left(-\gamma \left[P^{\pi^{w_{k-1}}} \Delta_{k-1} \right] (s, a) \right).$$

- 8: Minimize Bellman error for Q_θ weighted by w_k .
 $\theta_{k+1} \leftarrow \operatorname{argmin}_\theta \frac{1}{N} \sum_i^N w_k(s_i, a_i) (Q_\theta(s_i, a_i) - y_i)^2$.
 - 9: Minimize ADP error for training ϕ .
 $\phi_{k+1} \leftarrow \operatorname{argmin}_\phi \frac{1}{N} \sum_{i=1}^N (\Delta_\phi(s_i, a_i) - \hat{\Delta}_i)^2$.
 - 10: **end for**
-

Algorithm 2 ReMERT

- 1: Initialize Q-values $Q_\theta(s, a)$, a replay buffer μ , and a weight model κ_ψ .
 - 2: **for** step k in $\{1, \dots, N\}$ **do**
 - 3: Collect M samples using π_k , add them to replay buffer μ , sample $\{(s_i, a_i)\}_{i=1}^N \sim \mu$.
 - 4: Evaluate $Q_\theta(s, a)$ and $\kappa_\psi(s, a)$ on samples (s_i, a_i) .
 - 5: Compute target values for Q on samples:
 $y_i = r_i + \gamma \max_{a'} Q_{k-1}(s'_i, a')$.
 $\hat{a}_i = \arg \max_a Q_{k-1}(s'_i, a)$.
 - 6: **Optimize** κ_ψ **using**

$$L_\kappa(\psi) := \mathbb{E}_{\mathcal{D}_s} [f^*(f'(\kappa_\psi(s, a)))] - \mathbb{E}_{\mathcal{D}_t} [f'(\kappa_\psi(s, a))]$$
.
 - 7: **Compute** w_k **using**

$$w_k(s, a) \propto \frac{d^{\pi_k}(s, a)}{\mu(s, a)} \exp \left(-\mathbb{E}_{q_{k-1}(\tau)} \text{TCE}_c(s, a) \right).$$
 - 8: Minimize Bellman error for Q_θ weighted by w_k .

$$\theta_{k+1} \leftarrow \operatorname{argmin}_\theta \frac{1}{N} \sum_i^N w_k(s_i, a_i) (Q_\theta(s_i, a_i) - y_i)^2.$$
 - 9: **end for**
-

D Experiments

We now present some additional experimental results and experiment details which we could not present due to shortage of space in the main body.

D.1 Cumulative Recurring Probability on Atari Games

Table 1: The value of ϵ_π with different policies in Atari games.

	Initial (Random) policy	Policy at timestep 100k	Policy at timestep 200k
Pong	0.00	0.00	0.00
Breakout	0.00	0.00	0.00
Kangaroo	0.44	0.32	0.15
KungFuMaster	0.66	0.06	0.01
MsPacman	0.44	0.04	0.00
Qbert	0.02	0.05	0.00
Enduro	0.00	0.00	0.00

In Pong, Breakout and Enduro, ϵ_π keeps zero, so there is no error terms in such environments. For KungFuMaster and MsPacman, though ϵ_π is high for the initial policy, its value decreases rapidly as the policy updates. The error term in Kangaroo induces some error but ϵ_π is still much smaller than one. The experiment results imply we can ignore the error term in most reinforcement learning environments.

D.2 Illustrations on Stable Temporal Structure

We conduct an extra experiment in the GridWorld environment to support our claim that the trajectories have a stable temporal ordering of states. Fig. 1 shows an empirical verification of the stable temporal ordering of states property.

The result shows that the variance of distance to end in one state is not large and decreases fast in training process. This means the property is not a strong assumption and can be satisfied in many environments.

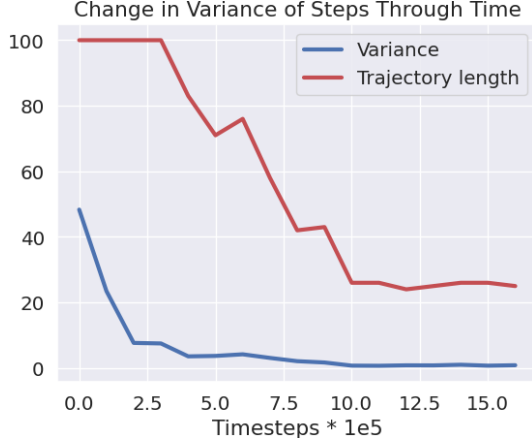


Figure 1: Change in variance of distance to end through time. For each timestep, the red line shows the average trajectory length in the last 500 states. The blue line shows the average variance of the last 500 states, where the variance for each state is calculated from its positions in their corresponding trajectories.

D.3 Description of Involved Environments

The Meta-World benchmark [?] includes a series of robotic manipulation tasks. These tasks differ from traditional goal-based ones in that the target objects of the robot. For example, the screw in the hammer task has randomized positions and can not be observed by RL agents. Therefore, Meta-World suite can be highly challenging for current state-of-the-art off policy RL algorithms. Visual descriptions for the Meta-World tasks are shown in Fig. 2. DisCor [?] showed preferable performance on some Meta-World tasks compared to SAC and PER [?], but the learning process is slow and unstable.

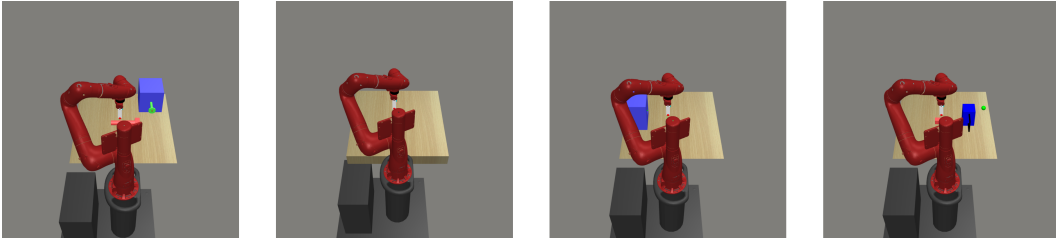


Figure 2: Pictures for Meta-World tasks hammer, sweep, peg-insert-side and stick-push.

D.4 Extended Results on Atari Environment

We evaluate ReMERN on an extended collection of Atari environments. As is shown in Tab. 2, ReMERN outperforms baseline methods in most of the environments.

D.5 Extended Evaluation on Gridworld

Aside from the FourRooms environment in Gridworld, we also conduct comparative evaluation on the Maze environment. The results are shown in Fig. 3. The Maze environment perfectly fits for our TCE-based prioritization, and TCE achieves the best performance among other methods.

D.6 The Relation Between Distance to End and $|Q_k - Q^*|$

In section D.5, the relationship between $|Q_k - Q^*|$ and distance to end has been shown in tabular environments. In this section, we explore the relationship in environments with continuous state and

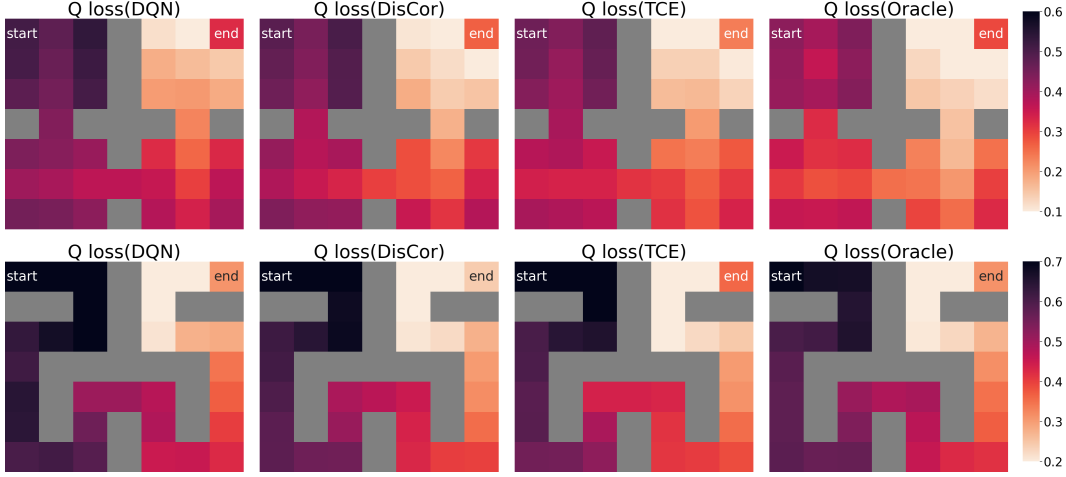


Figure 3: Extended evaluation results on Gridworld.

action spaces, i.e., Ant and Hopper tasks of MuJoCo environment. Since Q^* is inaccessible in these complex continuous control tasks, we approximate it by doing Monte-Carlo rollout using the best policy during training. The results are shown in Fig. 4.

The negative correlation between the two quantities is obvious in Ant-v2, but vague in Hopper-v2. It is because Hopper is a relatively easy task so that all state-action pair have small Q loss and don't have such correlation. The performance of ReMERT shown in Section 4 accords with this observation. ReMERT outperforms other algorithms in environments with a high correlation between the two quantities, and has a relatively poor performance in environments without such correlation.

D.7 Implementation Details

D.7.1 Algorithm Details

Weight Normalization To stabilize the prioritization, we apply normalization to the estimation of two terms: $\frac{d\pi_k(s,a)}{\mu(s,a)}$ and $\exp(-|Q_k - Q^*|)$.

Table 2: Extended experiments on Atari.

Environments	DQN(Nature)	DQN(Baseline)	PER(rank-b.)	ReMERT(Ours)
Assault	3395 ± 775	8260 ± 2274	3081	9952 ± 3249
BankHeist	429 ± 650	1116 ± 34	824	1166 ± 82
BeamRider	6846 ± 1619	5410 ± 1178	12042	5542 ± 1577
Breakout	401 ± 27	242 ± 79	481	223 ± 79
Enduro	302 ± 25	1185 ± 100	1266	1303 ± 258
Kangaroo	6740 ± 2959	6210 ± 1007	9053	7572 ± 1794
KungFuMaster	23270 ± 5955	29147 ± 7280	20181	35544 ± 8432
MsPacman	2311 ± 525	3318 ± 647	964.7	3481 ± 1350
Riverraid	8316 ± 1049	9609 ± 1293	10205	10215 ± 1815
SpaceInvaders	1976 ± 893	925 ± 371	1697	877 ± 249
UpNDown	8456 ± 3162	134502 ± 68727	16627	145235 ± 94643
Qbert	10596 ± 3294	13437 ± 2537	12741	14511 ± 1138
Zaxxon	4977 ± 1235	5070 ± 997	5901	5738 ± 1296

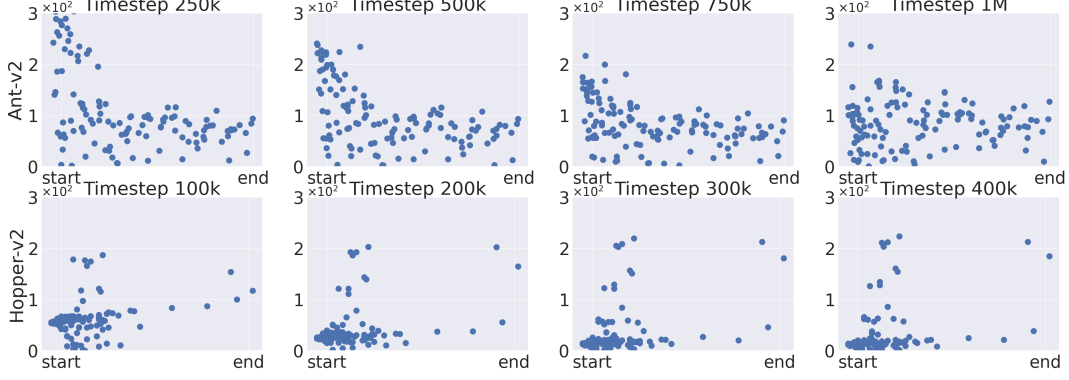


Figure 4: The relationship between $|Q_k - Q^*|$ and distance to end in two MuJoCo tasks (Ant and Hopper).

First, we introduce the normalization in calculating $\frac{d^{\pi_k}(s,a)}{\mu(s,a)}$, which aims to address the finite sample size issue. The normalization is:

$$\tilde{\kappa}_\psi(s, a) := \frac{\kappa_\psi(s, a)^{1/T}}{\mathbb{E}_{\mathcal{D}_s}[\kappa_\psi(s, a)^{1/T}]}$$

where \mathcal{D}_s is the slow buffer and T is temperature.

ReMERN uses Δ_ϕ to fit the discounted cumulative Bellman error. However, the Bellman error has different scales in various environments, leading to erroneous weight. We normalize it by dividing a moving average of Bellman error. The divisor is denoted as τ . Then the estimation of $\exp(-|Q_k - Q^*|)$ becomes

$$\exp\left(-\frac{\gamma [P^{\pi^{w_{k-1}}} \Delta_{k-1}](s, a)}{\tau}\right)$$

Truncated TCE TCE may suffer from a big deviation when $h_\tau^\pi(s, a)$ is too large or too small. To tackle this issue and improve the stability of the prioritization, we clip the output of TCE into $[b_1, b_2]$, where b_1 and b_2 are regarded as hyperparameters.

Baselines For the ReMERN and ReMERT algorithms in continuous action spaces with sensory observation, we alter the re-weighting strategy to $\frac{d^{\pi_k}(s,a)}{\mu(s,a)}$ and TCE approximation based on the source code provided by DisCor¹. For the algorithms in discrete action spaces with pixel observation, we employ the baseline Tianshou² [?] and add corresponding components.

D.7.2 Hyperparameter Details

The hyperparameters of our ReMERN and ReMERT algorithms include network architectures, learning rates, temperatures in on-policy reweight and DisCor, and the lower and upper bound in TCE algorithm. They are specified as follows:

- **Network architectures** We use standard Q and policy network in MuJoCo benchmark with hidden network sizes [256, 256]. In Meta-World we add an extra layer and the hidden network sizes are [256, 256, 256]. The networks computing Δ and κ have one extra layer than the corresponding Q and policy network.
- **Learning rates** The learning rate for continuous control tasks, including Meta-World, MuJoCo and DMC, is set to be 3e-4 for Q and policy networks alike. For Atari games, the learning rate is set to be 1e-4 and fixed across all environments.

¹<https://github.com/ku2482/discor.pytorch>

²<https://github.com/thu-ml/tianshou>

- **Temperatures** The temperature for weights related with $\frac{d^{\pi_k}(s,a)}{\mu(s,a)}$ is 7.5 and fixed across different environments. Also, DisCor has a temperature hyperparameter related to the output normalization of the error network. We keep it unchanged in the Meta-World and DMC benchmark, and divide it by 20 in MuJoCo environments to make it compatible with on-policy prioritization weights.
- **Bounds in TCE** We select time-adaptive lower and upper bounds for TCE. The lower bound rises from 0.4 when training begins to 0.9 when it ends, and the upper bound drops from 1.6 to 1.1 accordingly. The bounds are fixed across different environments.
- **Random Seeds** In MuJoCo, Meta-World and DMC benchmarks, we run each experiment with four random seeds. The results are plotted with the mean of the four experiments. In Atari games, we run experiments with three random seeds and select the one with max return.